NASA Technical Memorandum 4631

NASA Dryden Flow Visualization Facility

John H. Del Frate

May 1995

NASA Technical Memorandum 4631

NASA Dryden Flow Visualization Facility

John H. Del Frate
Dryden Flight Research Center
Edwards, California

National Aeronautics and
Space Administration

Office of Management

Scientific and Technical
Information Program

1995

CONTENTS

Page

ABSTRACT 1

INTRODUCTION 1

NOMENCLATURE 2

FACILITY DESCRIPTION 3
  Vertical Test Section Flow Specifications 4
  Horizontal Test Section 6

FLOW VISUALIZATION TECHNIQUES 6
  Dye Tracer 6
  Laser Light Sheet 8
  Shadowgraph Photography and the Hydraulic Analogy 10

QUANTITATIVE MEASUREMENT TECHNIQUES 11

MODEL SUPPORT SYSTEMS AND TEST EQUIPMENT 12
  Blowing and Suction 14
  Moving Ground Plane 15
  Cameras 16

MODELS 16

FLOW VISUALIZATION FACILITY ENCLOSURE 21

FLOW VISUALIZATION FACILITY STAFF 21

SUMMARY 21

APPENDIX — VERTICAL TEST SECTION CALIBRATION SYSTEM 23

REFERENCES 25

ABSTRACT

This report describes the Flow Visualization Facility at NASA Dryden Flight Research Center, Edwards, California. This water tunnel facility is used primarily for visualizing and analyzing vortical flows on aircraft models and other shapes at high-incidence angles. The tunnel is used extensively as a low-cost, diagnostic tool to help engineers understand complex flows over aircraft and other full-scale vehicles. The facility consists primarily of a closed-circuit water tunnel with a 16- × 24-in. vertical test section. Velocity of the flow through the test section can be varied from 0 to 10 in/sec; however, 3 in/sec provides optimum velocity for the majority of flow visualization applications. This velocity corresponds to a unit Reynolds number of 23,000/ft and a turbulence level over the majority of the test section below 0.5 percent. Flow visualization techniques described here include the dye tracer, laser light sheet, and shadowgraph. Limited correlation to full-scale flight data is shown.

INTRODUCTION

As a flow visualization medium, water has historically played a significant role in understanding the effects and characteristics of a fluid flowing past a body. Use of water as a scientific tool to visualize fluid flow dates back to Leonardo da Vinci (1452–1519). Historical and current applications, limitations of water tunnels, and descriptions of various representative water tunnel facilities and of typical flow phenomenon studies for which such facilities are used have been reported.[1, 2]

More recently, water tunnels have become an important tool for studying complex flows and flow field interactions on aircraft shapes generating strong vortex flows. Flow visualization in water tunnels is useful in determining vortex strength, location, and control methods. To assist researchers in the understanding of the aerodynamics of aircraft configurations with strong vortex flows, particularly at high angles of attack, a water tunnel facility called the Flow Visualization Facility (FVF) was built at the NASA Dryden Flight Research Center, Edwards, California. The design was patterned after the Northrop Corporation Water Tunnel located in Hawthorne, California.[1–6]

The FVF has been successfully used many times over the years since it became operational in 1983. Some years as many as 25 test entries were logged. Principal use of this facility has been the study of high-angle-of-attack aerodynamics—the purpose for which it was built. In this capacity, the FVF yields results which compare well to flight data. One such comparison was made taking measurements from the vortex generated by the leading-edge extension on an F-18 airplane (McDonnell Douglas Aerospace, St. Louis, Missouri, and Northrop Corporation, Newbury Park, California).[7]

Figure 1 shows the longitudinal location of the vortex breakdown as a function of angle of attack from flight, FVF, and three wind tunnels. Although the Reynolds number in the FVF is orders of magnitude lower than that of the wind tunnel data sets, the FVF results compare well with these data sets.

Other uses for the facility include studying how such flight hardware as pylons, probes, antennas, parachutes, and experimental fixtures affects flow. In addition, the FVF has proved helpful in determining the best locations for emitting smoke for flow visualization in several NASA flight programs.

As an ancillary benefit, the FVF provides a powerful instructional aid for engineers and engineering trainees who are unfamiliar with what flow looks like and how it behaves over a broad variety of conditions. Although primarily designed as a facility where flow is studied qualitatively, the FVF has been used in quantitative studies as well. Such techniques as laser doppler velocimetry and hot film anemometry have been employed successfully in the FVF.

Access to the FVF can be restricted for testing of classified models and lasers. This facility is staffed with experienced craftsmen and engineers. This staff can provide various levels of support in the areas of design, fabrication, instrumentation, and testing.

This document describes the FVF and its capabilities, the supporting systems, and the test techniques commonly employed here. Flow characteristics are also described. This document serves as a test facility reference publication and will be updated periodically. Use of tradenames or names of manufactures in this document does not constitute an official endorsement of such products or manufacturers, either expressed or implied, by the National Aeronautics and Space Administration.

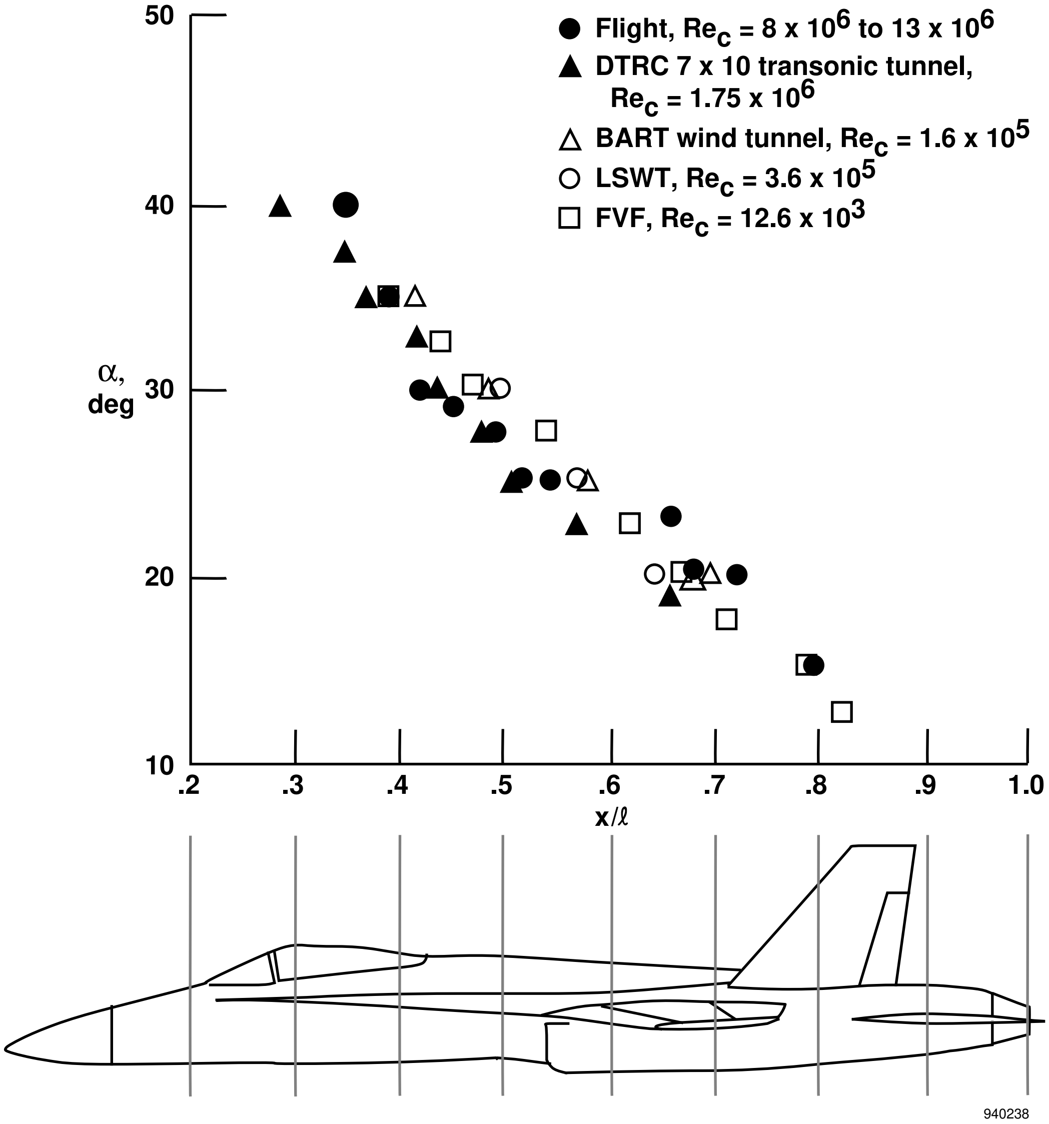

Figure 1. Comparison of F-18 airplane leading edge extension vortex core breakdown location between flight, water tunnel, and wind tunnel facilities.

NOMENCLATURE

BART	Basic Aerodynamic Research Tunnel, Langley Research Center, Hampton, Virginia
CTA	constant temperature anemometer
DTRC	David Taylor Research Center, Annapolis, Maryland
FVF	Flow Visualization Facility
LSWT	Low Speed Wind Tunnel, McDonnell Douglas Aerospace, St. Louis, Missouri
O.D.	outer diameter
RMS	root mean square
Re_c	Reynolds number based on the mean aerodynamic chord
T	turbulence intensity, T = RMS of $Vel_{unsteady}$, in/sec
$T\%$	Percent of turbulence, $T\% = T/Vel_{avg} \times 100$
Vel	vertical velocity component in the flow through the vertical test section, in/sec
Vel'	dye pulse speed, in/sec
Vel_{avg}	vertical velocity component in the flow through the vertical test section as determined using hot film anemometer data averaged over 10 sec, in/sec

Vo	hot film probe output voltage level, V
Vo'	output voltage at the center probe position averaged over 10 sec, V
Vo_{avg}	hot film probe output voltage level averaged over 10 sec, V
$Vo_{unsteady}$	the unsteady component of the raw voltage signal from the hot film probe, V
$Vel_{unsteady}$	the unsteady vertical velocity component in the flow through the vertical test section, in/sec
V/STOL	vertical or short takeoff and landing

FACILITY DESCRIPTION

The original design of the FVF was conceived by Northrop Corporation, Hawthorne, California. The overall design was driven by the requirement that the water tunnel take up a minimum of floor space, hence the vertical orientation of the structure.

Figure 2 shows the FVF. This closed-return water tunnel can operate continuously. The water tunnel tank is the most prominent part of the facility and is made of stainless steel supported by a wood and steel superstructure. Water flows into the settling chamber of the tank through a 12 in. outer diameter (O.D.) pipe which has small holes around its perimeter. These holes reduce the turbulence in the water flow imparted by the pump and the plumbing action. The water rises through the settling chamber and transitions to horizontal movement through two 2-in. thick honeycomb flow straighteners. The flow then turns downward and passes through another 2-in. thick honeycomb flow straightener before proceeding down through the vertical test section.

Figure 3 shows the vertical test section. This 72 in. long section has a cross-section of 16 in. × 24 in. The 2-in. thick clear acrylic plastic walls facilitate a 360° view of tests in progress. A round aluminum door provides access to the interior. This door is 16 in. in diameter and located on the side of the test section.

A backflow plate perforated with 0.25-in. holes is located at the bottom of the test section. This plate was installed to make the flow velocity profile more nearly uniform across the test section. The flow proceeds through the holes and then enters the return line which is nominally 8-in. O.D. The return line completes the circuit by feeding water back through a pump to the settling tank. Specifications on the flow through the vertical test section are presented in the next section.

A centrifugal pump forces the water around the circuit. The pump is powered by a 15-hp electric motor.

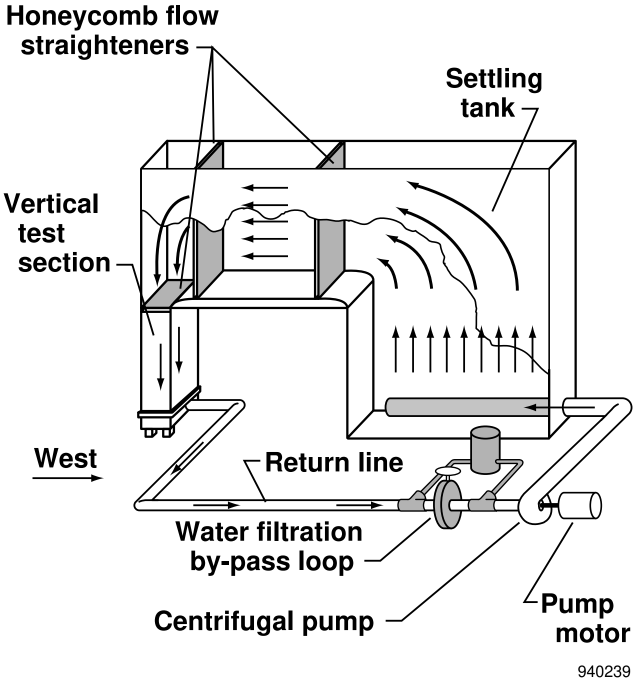
Honeycomb flow straighteners
Settling tank
Vertical test section
West
Return line
Water filtration by-pass loop
Centrifugal pump
Pump motor
940239

Figure 2. Flow Visualization Facility.

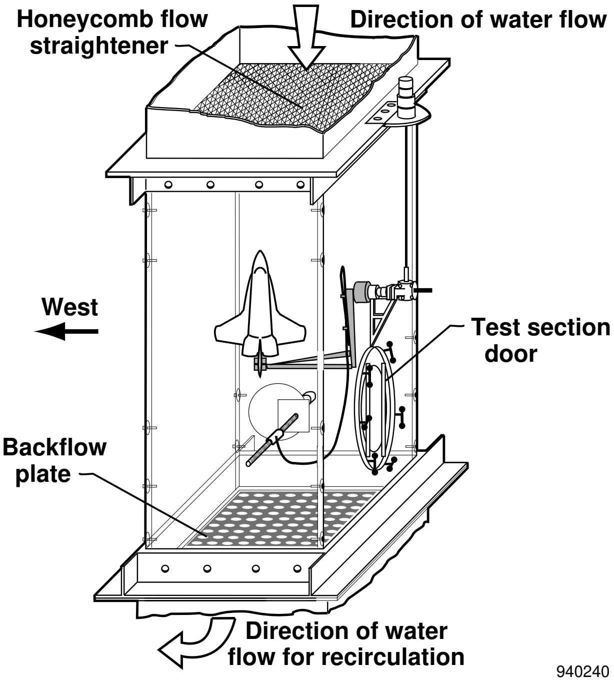
Honeycomb flow straightener
Direction of water flow
West
Test section door
Backflow plate
Direction of water flow for recirculation
940240

Figure 3. Vertical test section.

Pumping rates are varied using an eddy current clutch which varies the pump revolutions per minute.

A by-pass loop exists along the return line (fig. 2). Water is cleaned by pumping it through the by-pass loop, a swimming pool pump, and a diatomaceous earth filter system.

Vertical Test Section Flow Specifications

The water tunnel is typically operated at a water level 12 in. from the top of the tank. Flow measurements conducted with water levels of less than 12 in. have shown that significant deterioration in the quality of the velocity profiles and turbulence levels occurs. The lower the water level, the worse the deterioration. Flow velocity and turbulence through the vertical test section are determined using a hot film probe with a constant temperature anemometer.[8,9] The appendix provides a detailed description of the measurement procedure. The probe is positioned at 10 locations across the test section at a height of 27 in. above the backflow screen (figs. 4(a) and 4(b)). This probe is approximately 18 in. downstream of the location at which most models are tested. Measurements are not made near the north and south walls.

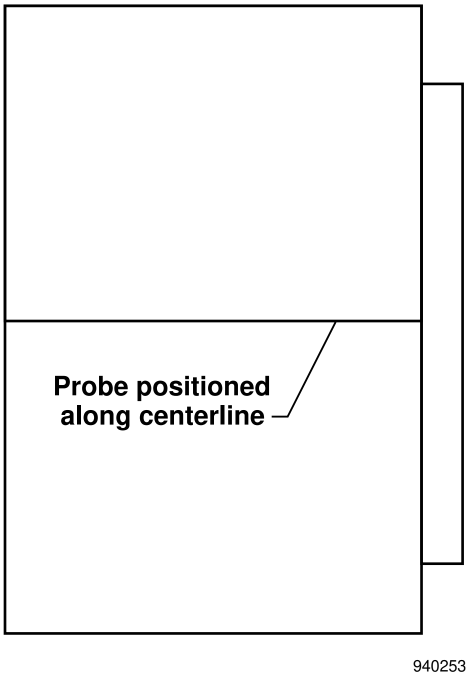
Probe positioned along centerline
940253

(a) Top view.

Figure 4. Hot film probe measurement locations in the vertical test section.

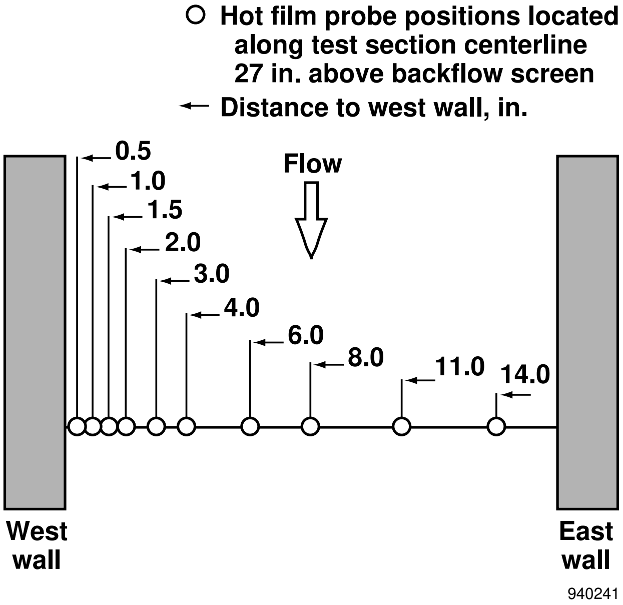
○ Hot film probe positions located along test section centerline 27 in. above backflow screen
← Distance to west wall, in.
0.5
1.0
1.5
2.0
3.0
4.0
6.0
8.0
11.0
14.0
Flow
West wall
East wall
940241

(b) Side view.

Figure 4. Concluded.

Flow velocity is determined at each location for pump settings of 100, 200, 300, 400, 500 and 550 rpm, which is the full range of revolutions per minute for the motor and pump set-up. The following table shows the velocity achieved at the test section centerline for these pump settings at a water level 12 in. from the top of the tank:

Pump, rpm	Velocity at test section centerline, in/sec
100	1.88
200	3.48
300	5.76
400	7.64
500	9.55
550	10.25

Figure 5(a) shows the velocity profile across the test section for each of the pump settings for a water level 12 in. from the top of the tank. These data show that the velocity profile is generally flat for the pump settings

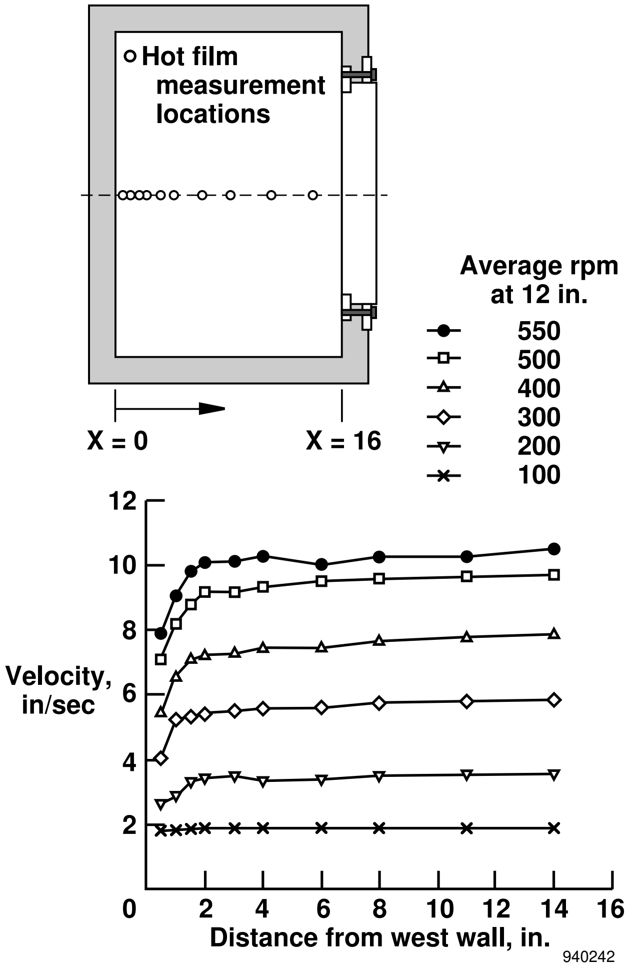

(a) Velocity as a function of distance from the west wall.

Figure 5. Flow quality across vertical test section at a water level 12 in. from the top of the tank.

below 550 rpm. Note that the velocities within 2 in. of the west wall are less than the remainder of the velocities recorded. The decreased velocities are indicative of the wall boundary layer. This layer exists at the other three walls as well; however, no measurements were conducted at those locations. As speed increases, the boundary layer grows to approximately 2 in. thick on the west wall. Velocity profiles near the east wall appear to be flatter than those on the west wall. This difference indicates a thinner boundary layer on the east wall. Ideally, velocities measured at 2 and 14 in. from the west wall should be the same. In this case, velocity at the 2-in. position is less because a flow separation is believed to exist over the curved contraction surface on the west side of the inlet to the vertical test section.

Practical experience has shown that the best flow visualization results are observed at approximately 200 rpm, which yields a test section velocity slightly above 3 in/sec. At this setting, the velocity profile varies no more than 0.18 in/sec outside of the boundary layer.

The hot film anemometer data lent itself particularly well to determining the percent of turbulence, *%T*, in the test section. Figure 5(b) shows percent of turbulence levels corresponding to the data presented in figure 5(a). At 200 rpm, omitting the boundary layer, percent of turbulence remains less than 0.5 percent. As pump revolutions per minute increase, percent of turbulence increases. With the exception of the measurements near the west wall, percent of turbulence values stay near or below 1.0 percent. For the same reasons that the flow velocities near the west and east walls are not the identical, percent of turbulence measured at the

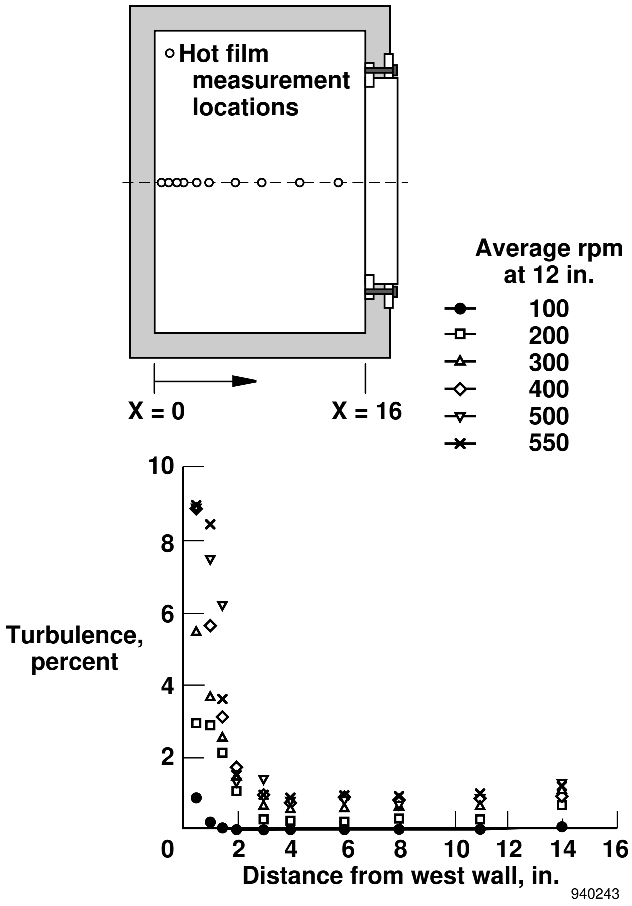

(b) Percent of turbulence as a function of distance from the west wall.

Figure 5. Concluded.

2-in. position is higher than that measured at the 14-in. position. Again, flow separation is believed to exist over the curved contraction surface on the west side of the inlet to the vertical test section.

Horizontal Test Section

Simple tests can be conducted in the horizontal test section. This section is the upper channel of the water tunnel tank between the two flow straighteners where the flow moves horizontally before turning downward to go through the vertical test section (fig. 6(a)). This test section functions either as a free-surface channel or as a water table by using a sluice gate (fig. 6(b)). The channel is 24 in. wide and 77.5 in. high. Flow rates vary with water level and pump speed. When used, sluice gate position also causes these rates to vary. A maximum flow rate of approximately 168 in/sec has been achieved using the sluice gate. Visual and physical access to the horizontal test section is limited to that available from above. Flow quality for this test section has not been quantified.

FLOW VISUALIZATION TECHNIQUES

Flow visualization techniques successfully employed in the FVF are presented in the following subsections. Although all of these techniques have merit, by far, the dye tracer technique is used more often than the others.

Dye Tracer

The dye tracer technique consists simply of emitting dye through flush ports, external tubes, probes, or other means such that the dye is entrained in the flow field of interest thereby revealing the flow structure.[10,11] Two- and three-dimensional flow structures surrounding a body are routinely observed and analyzed in the FVF using this technique. Figures 7 and 8 show examples of models using this technique. Models are usually painted white for best contrast with the colored dye.

The dye supply system consists of six pressurized dye containers mounted outside the test section with dye lines running to the test section (fig. 9). Dye lines are brought into the vertical test section through the door on the side of the test section. The dye consists of commercially available, diluted, vegetable food coloring. Multiple colors can be used for flow identification. The rate of dye flow is regulated using a needle valve on each container. Depending on the model configuration and test requirements, each main dye line can be routed to many smaller lines through manifolds. As many as 120 dye lines have been operated simultaneously in this way.

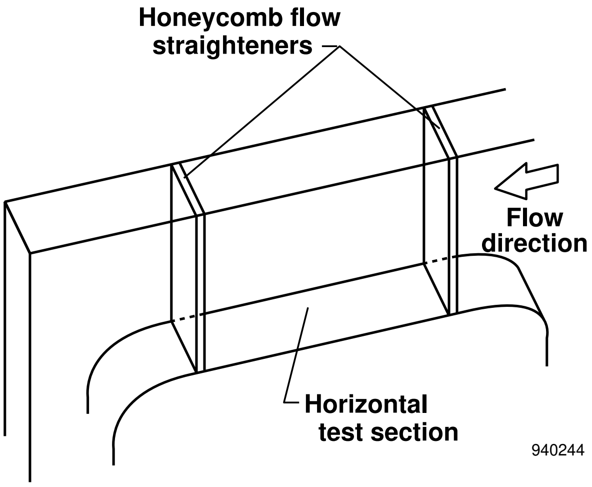

(a) Normal configuration.

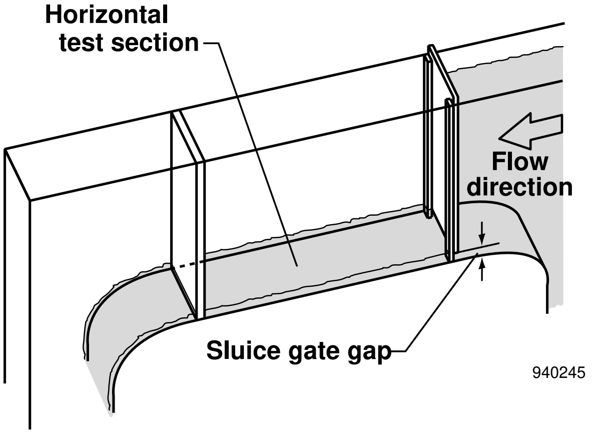

(b) Sluice gate configuration.

Figure 6. Horizontal test section.

Models are typically fabricated with internal dye lines which lead to flush ports on the model surface. The dye is emitted into the flow field through ports on the model surface. Dye can also be supplied to a dye port external to a model. For example, a dye source can be installed upstream of a model. When the dye proceeds downstream, it is entrained in a particular region of interest.

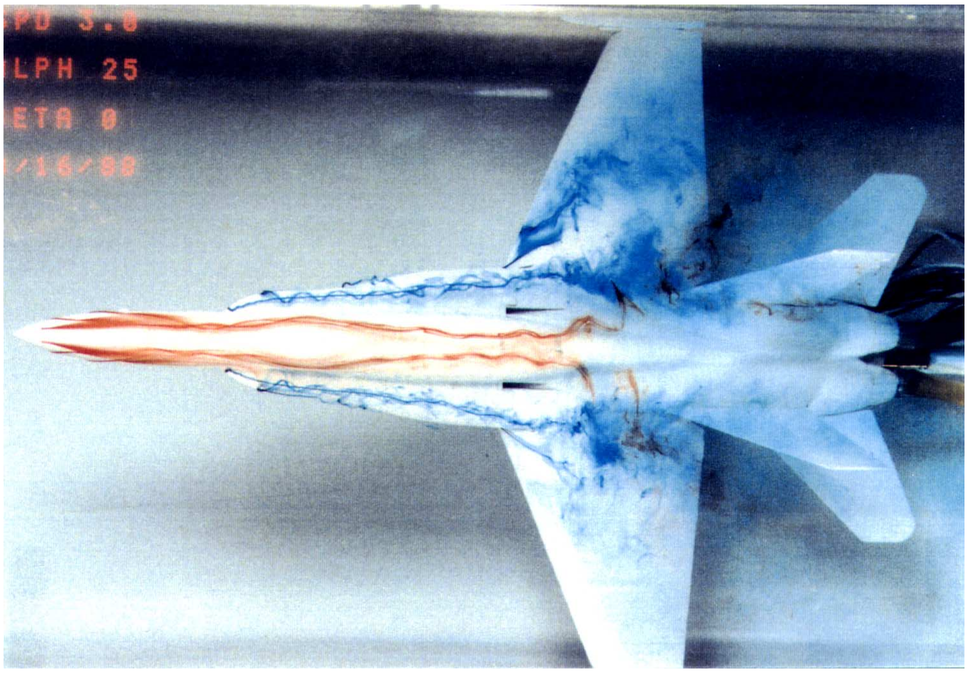

Figure 7. Side view of an F-18 model operating with the dye tracer technique in the vertical test section.

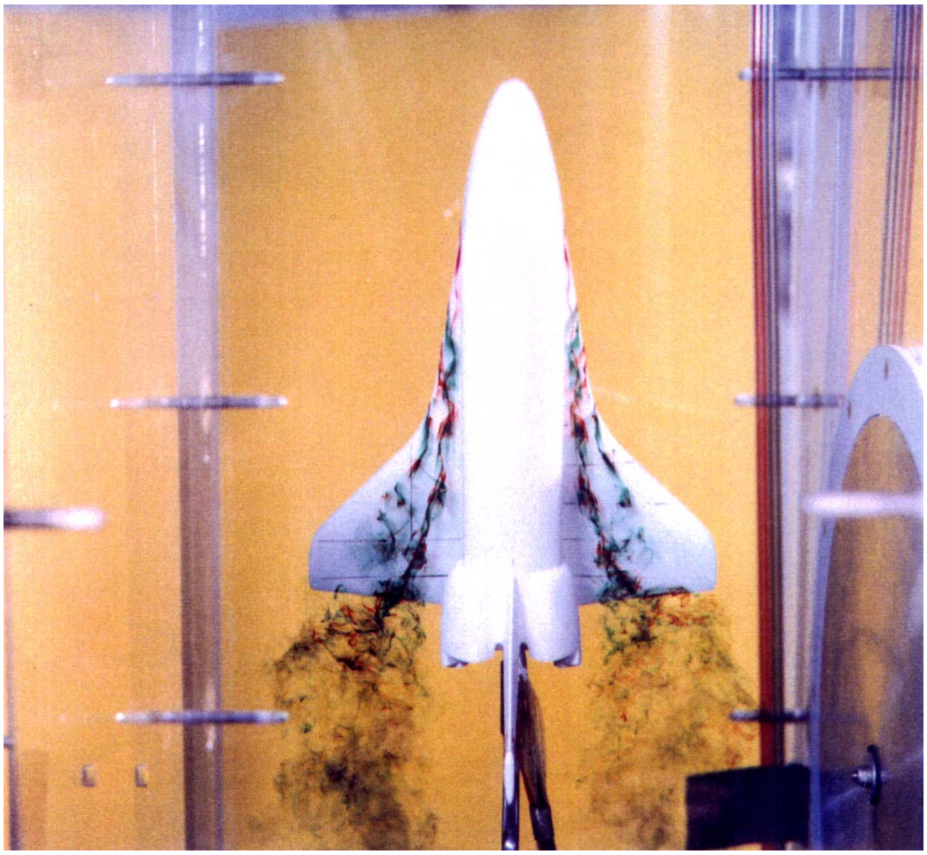

Figure 8. Top view of a shuttle model operating with the dye tracer technique in the vertical test section.

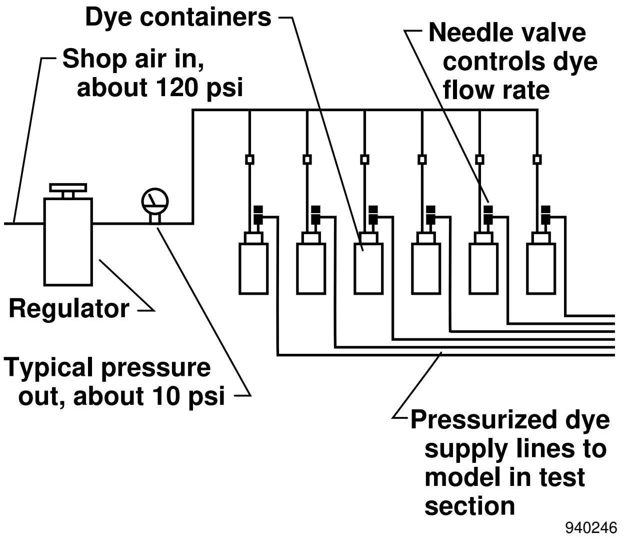
Dye containers
Shop air in, about 120 psi
Needle valve controls dye flow rate
Regulator
Typical pressure out, about 10 psi
Pressurized dye supply lines to model in test section
940246

Figure 9. Schematic of dye supply system.

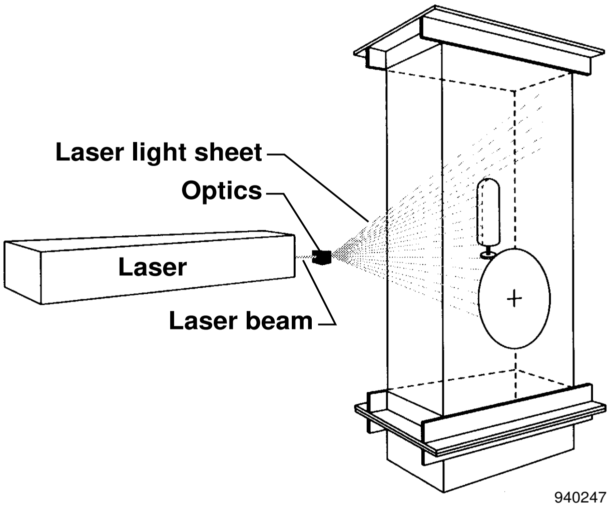
Laser light sheet
Optics
Laser
Laser beam
940247

Figure 10. Laser light sheet system

Laser Light Sheet

A sheet of light to illuminate a particular plane to show cross-sections of the flow structure has been successfully used in the FVF. The technique is similar to the vapor screen technique that is used in wind tunnels. An argon–ion laser provides the light source. A cylindrical lens converts the beam to a narrow sheet of light. Figure 10 shows a schematic of the set-up. The light sheet is positioned in the plane of interest, and the flow is seeded with a tracer material. This technique results in a visible representation of the streamlines at this cross-section. By repositioning the light sheet, other two-dimensional slices of the flow field can be viewed.

Two tracer materials are commonly used with this technique.[12,13] One is fluorescein disodium, a fluorescent dye which appears bright yellow-green when illuminated by the ultraviolet light generated by the argon–ion laser. This dye dissolves easily in water and is injected into the flow field in the same way as the vegetable food-coloring dyes.

Figure 11(a) shows a schematic of a cylindrical model with a trailing disk which was tested using the laser light sheet technique. Figure 11(b) shows flow observed during the test. This test revealed a well-formed, toroidal vortex between the base of the body and the trailing disk. The laser light sheet technique enabled observation of the internal structure of the vortex by providing a cross-sectional view.

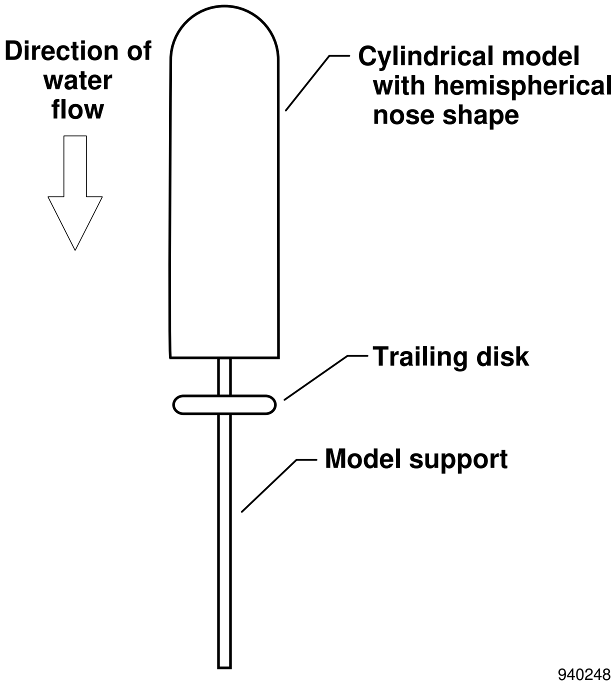
Direction of water flow
Cylindrical model with hemispherical nose shape
Trailing disk
Model support
940248

(a) Model description.

Figure 11. Comparison of tracer light sheet flow visualization technique on a cylindrical model.

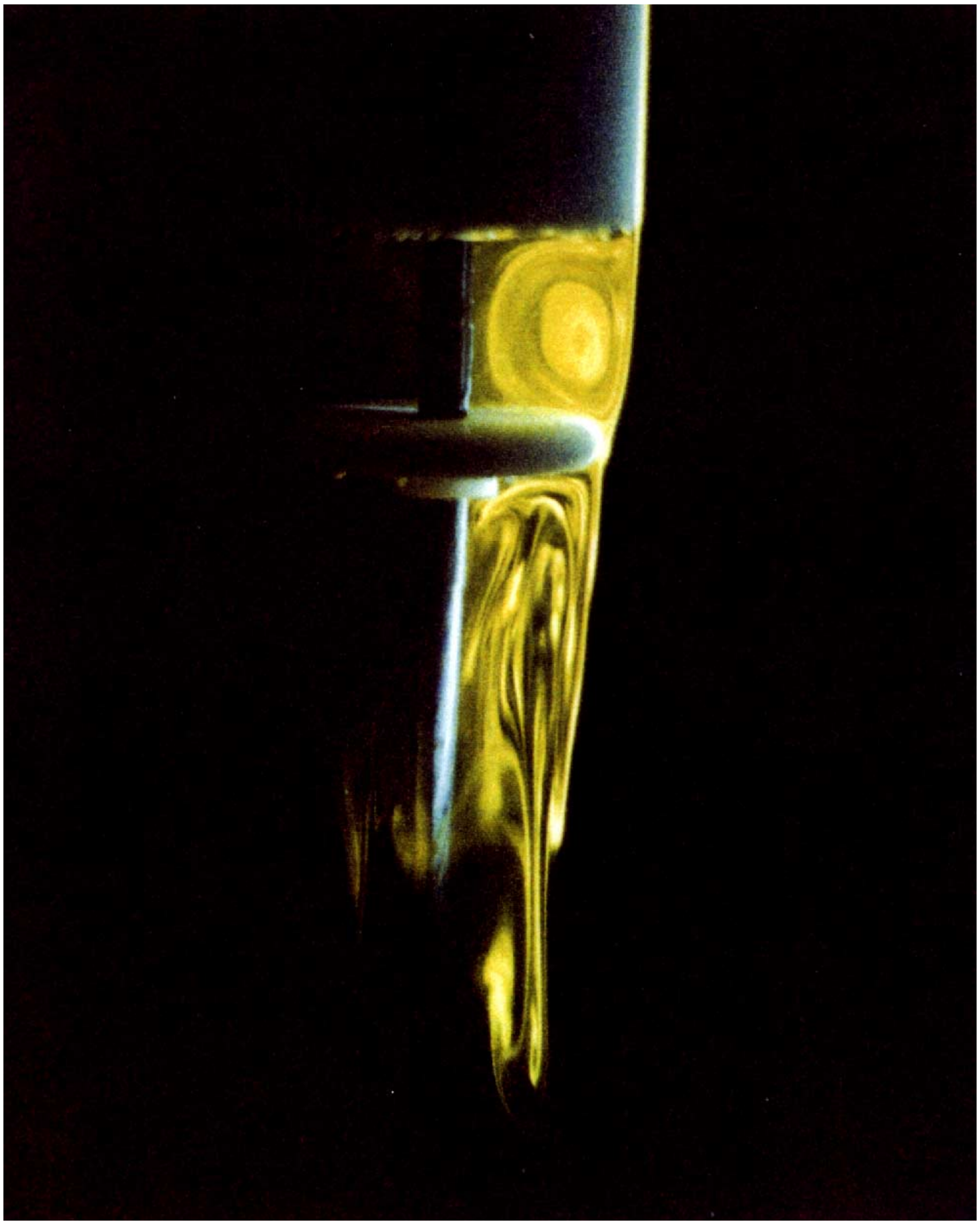

(b) Tracer material: Fluorescein sodium dye.

Figure 11. Continued.

Aluminum powder, the other tracer material commonly used with the laser light sheet, is mixed as evenly as possible in the entire water tunnel tank. The individual aluminum particles reflect the laser light, yielding streaks on a photographic negative or on video. In this case, the visible blue and green wavelengths of the argon–ion laser light are used. Streak length depends on local flow velocity and camera exposure duration. The streaks approximate the flow streamlines in the plane of light.

Figure 11(c) shows a test using the aluminum particles with the model shown in figure 11(a). Note that the back side of the donut-shaped vortex in figures 11(b) and 11(c) is not visible because the rod attaching the disk to the body is blocking the laser light sheet.

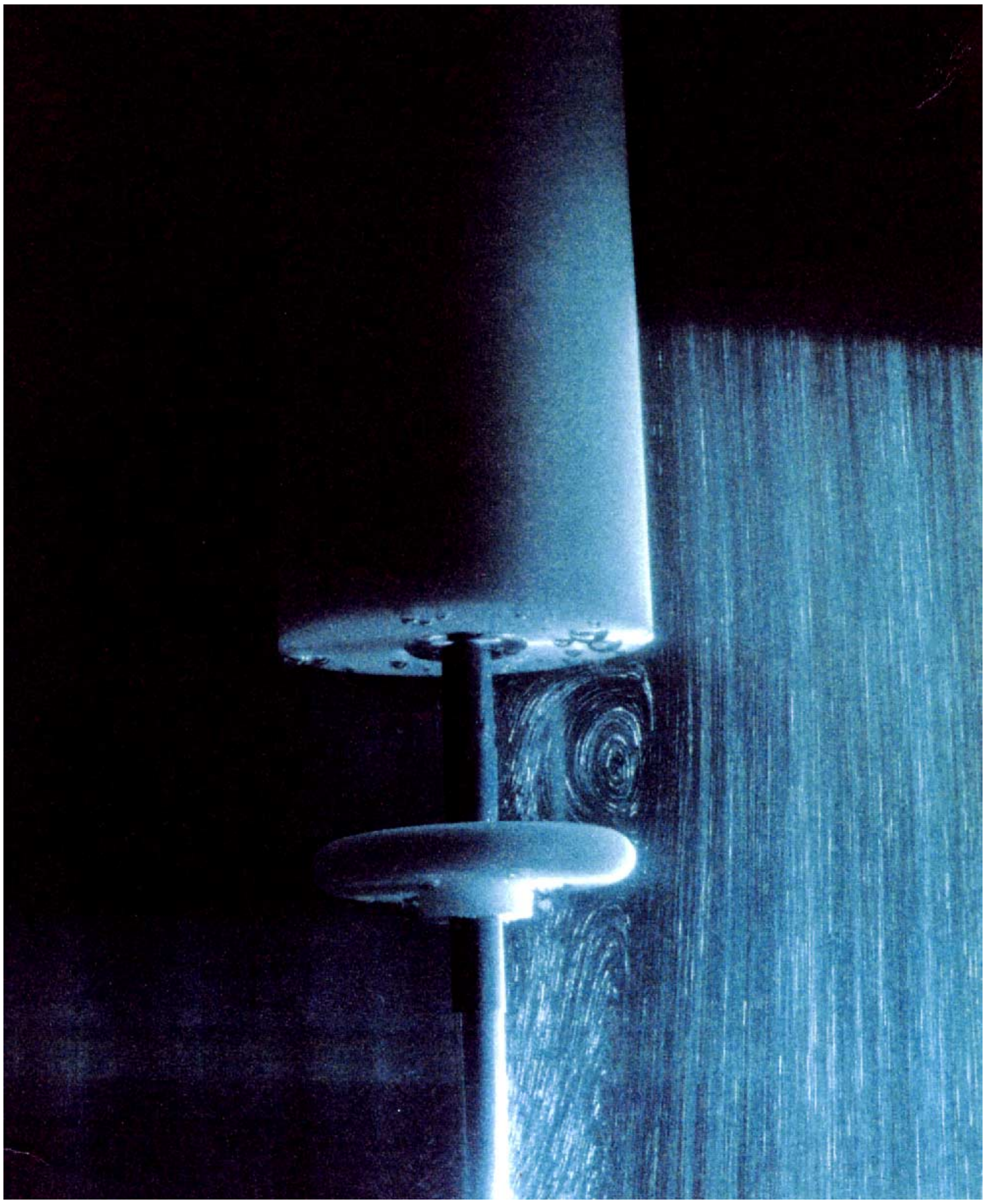

(c) Tracer material: Aluminum powder.

Figure 11. Concluded.

Aluminum powder is not neutrally buoyant and may not follow streamlines exactly. Qualitative results from using aluminum powder appear to differ from those obtained using fluorescent dye because the particles disperse throughout the water, allowing the complete flow field to be viewed in two-dimensional slices. With fluorescent dye, the flow field can be viewed only where the dye exists. On the other hand, use of the dye allows the user to observe specific flow phenomenon, such as a vortex, with increased detail.

Shadowgraph Photography and the Hydraulic Analogy

A variation of shadowgraph photography has been employed in the FVF in conjunction with the hydraulic analogy.[14–18] The normal approach in shadowgraph photography to study two-dimensional flow is to backlight a model and the resulting flow pattern. The shadow of the model and of the flow pattern falls on a ground glass sheet where it can be photographed.

The variation of shadowgraph photography used in the FVF was developed for use with the hydraulic analogy where the horizontal test section is used as a free surface water table. Briefly, this technique allows for the visualization of the hydraulic jump which is analogous to shock waves, such as those experienced by aircraft travelling supersonically or hypersonically.[15, 16] Two-dimensional models are placed on the bottom of the channel. The resulting wave form is similar to that of supersonic and hypersonic velocities, depending on the flow rate. The flow rate is controlled by a sluice gate upstream of the test section (fig. 6(b)), water height, and pump motor speed.

Visual and physical access is limited to the top in the horizontal test section, so backlighting the model and flow field is impossible. Instead, the floor of the channel was painted white, so the shadows cast on it from the wave forms on the water surface could be photographed. The camera and lights are situated above the channel. Figures 12(a) and 12(b) show test results of a generic hypersonic model using this technique. Figure 12(a) shows simulated Mach 2.15 flow, and figure 12(b) shows simulated Mach 4.10 flow. The simulated Mach number flow is determined by placing wedge models in the flow for which the shock wave pattern is known over a range of Mach numbers.

QUANTITATIVE MEASUREMENT TECHNIQUES

The FVF was primarily designed to conduct qualitative flow visualization research and that has been its main use. However, some quantitative measurement techniques have been used in the FVF on occasions and are briefly mentioned here. Velocity has been measured using a one-, two-, and three-component laser doppler velocimeter and a laser transit anemometer.[19–22]

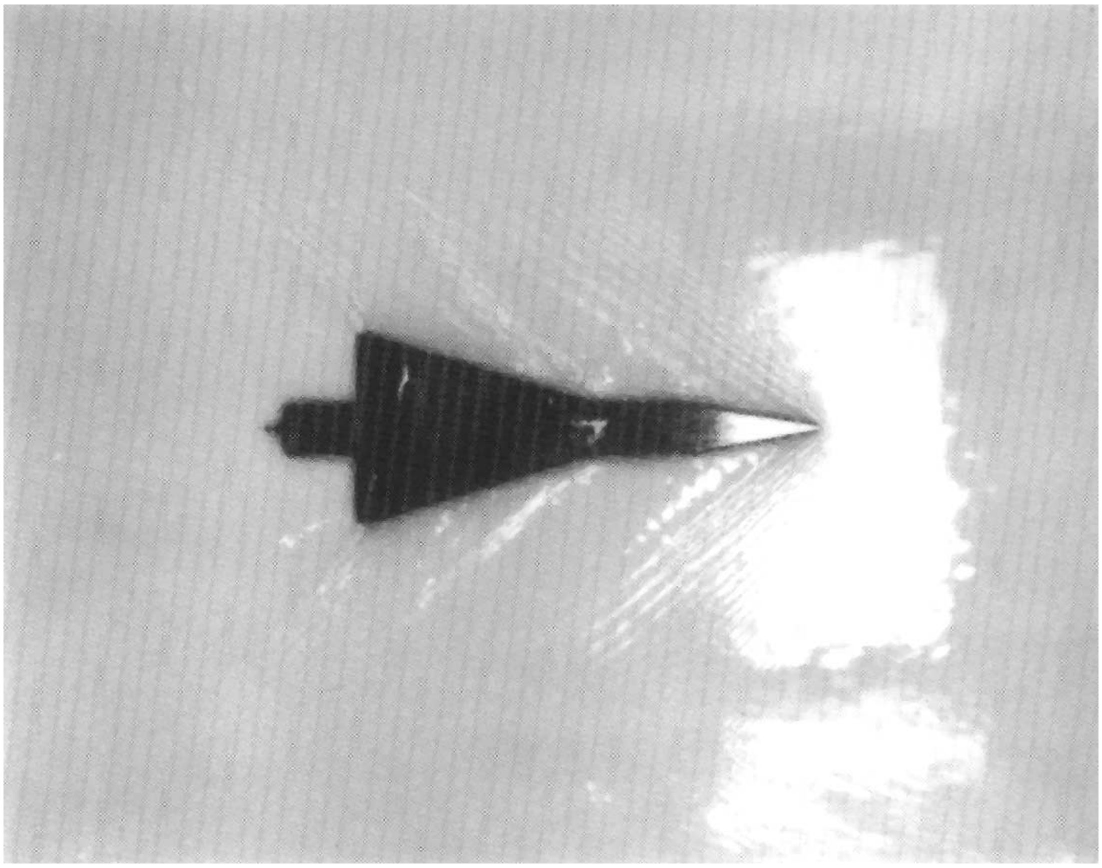

(a) Simulated Mach 2.15.

Figure 12. Two-dimensional models using the hydraulic analogy to simulate supersonic flow.

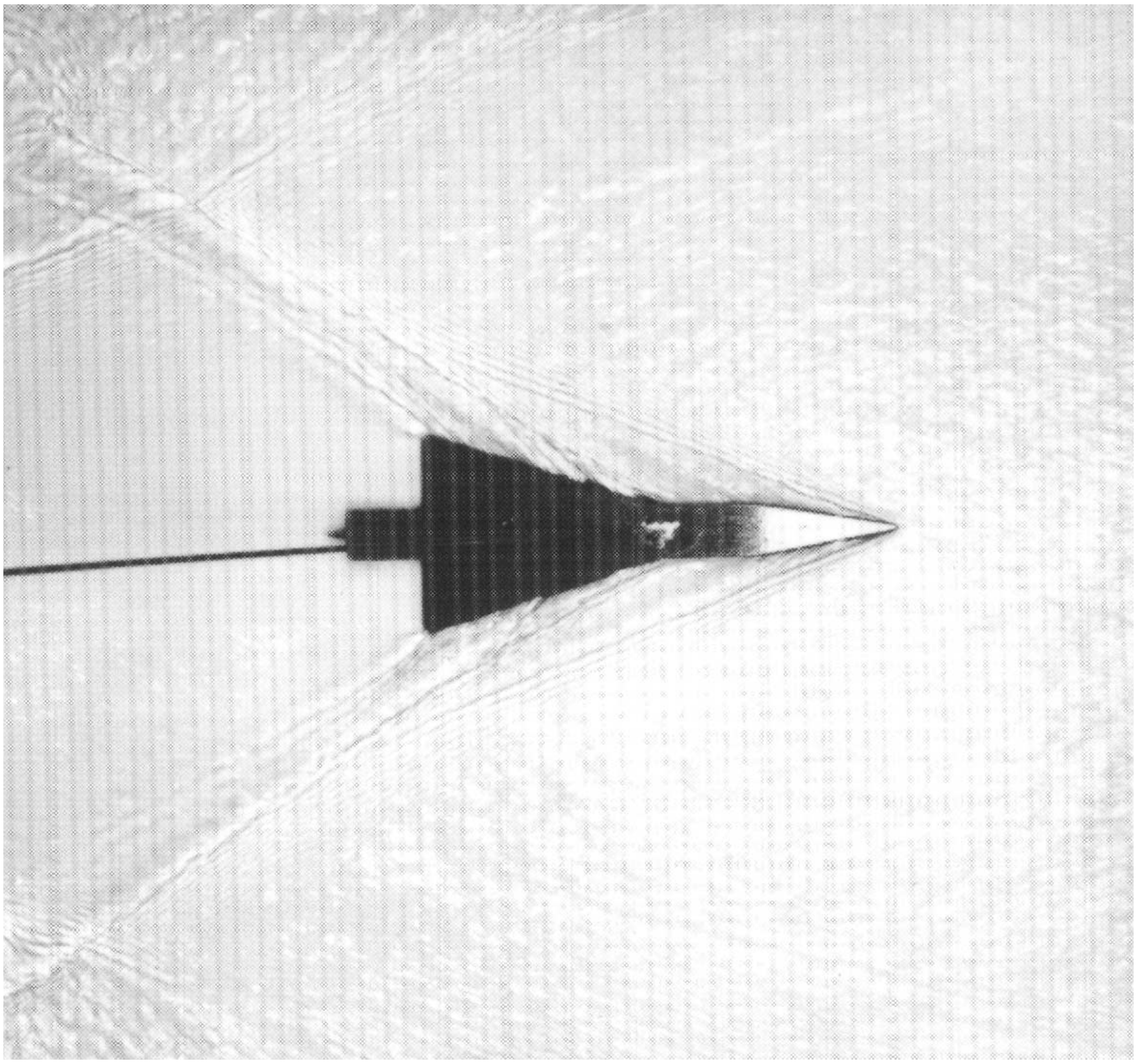

(b) Simulated Mach 4.10.

Figure 12. Concluded.

Hot film anemometry has also been used to measure velocity and turbulence in the flow and to study flow frequency content.[23]

The Vertical Test Section Flow Specifications subsection and the appendix provide additional information regarding hot film anemometry. Strain gauges have shown substantial promise for the measuring forces and moments.[24,25] Research in this area is ongoing.

MODEL SUPPORT SYSTEMS AND TEST EQUIPMENT

Research requirements dictate the manner in which the model is supported and manipulated during the test. A great deal of flexibility is maintained in the FVF to accommodate a large variety of tests. Although many ways to support test models exist, the FVF has available a standard system which is used to support aircraft models most of the time.

Figures 13(a) and 13(b) show the model support system that is most commonly used in the vertical test section. This system was designed to vary the pitch and yaw of the model from the exterior of the vertical test section while the FVF is operating. Pitch range of the model support system is ±90° or less, depending on model length. The yaw mechanism limits the yaw angle to approximately ±13° or less, depending on model length and wingspan.

Dimensions of two typically sized models are provided herein to give guidance in model size determination for use on the standard model support system. The first example is a 1 ⁄ 48 scale model of an F-117 airplane. The model is 15.75 in. long with an additional 1.25-in. sting support attached from the model rear. The wingspan is 10.75 in. This model could be yawed and

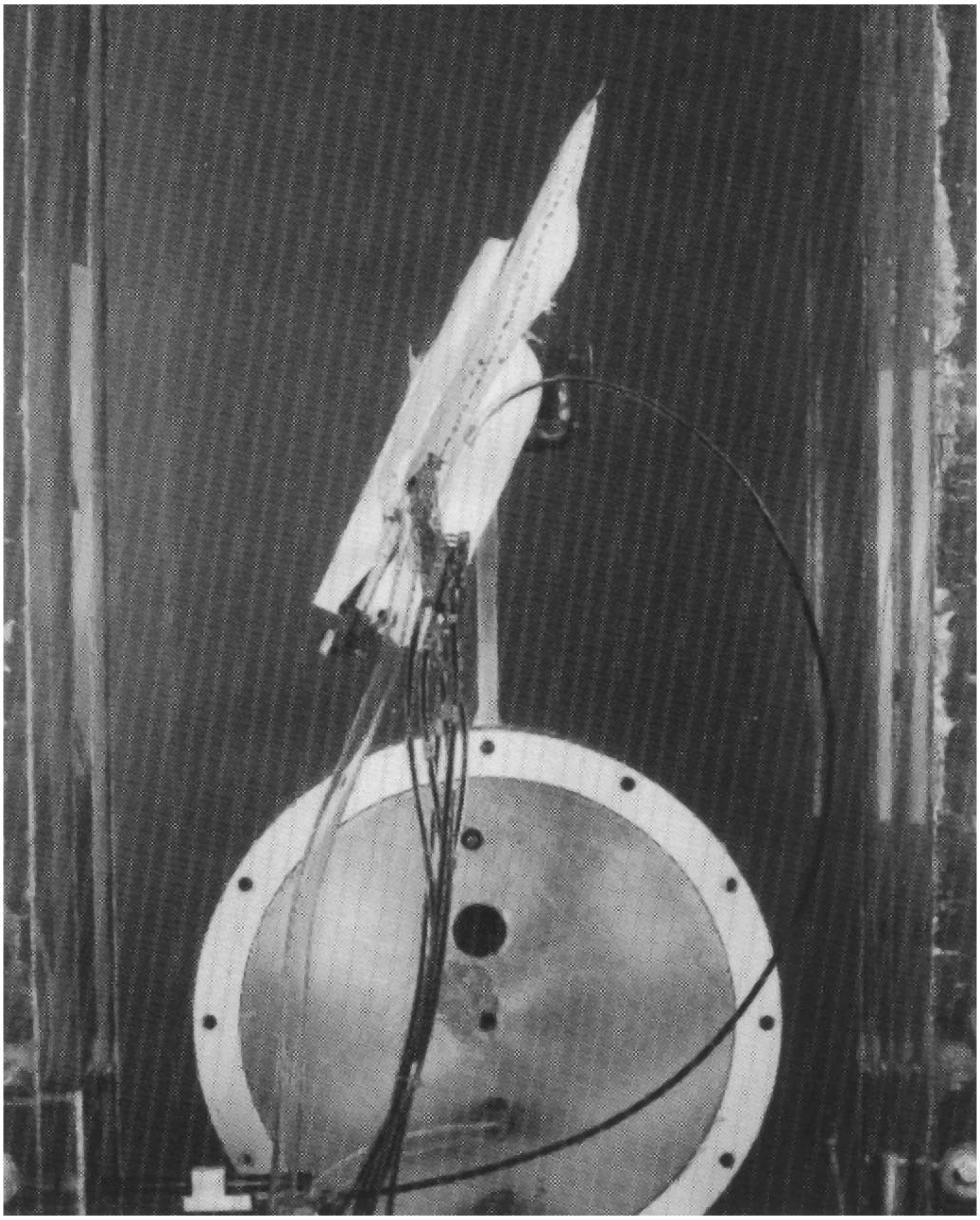

EC9442399-10

(a) View from the pitch axis.

Figure 13. Model support system most commonly used in the vertical test section.

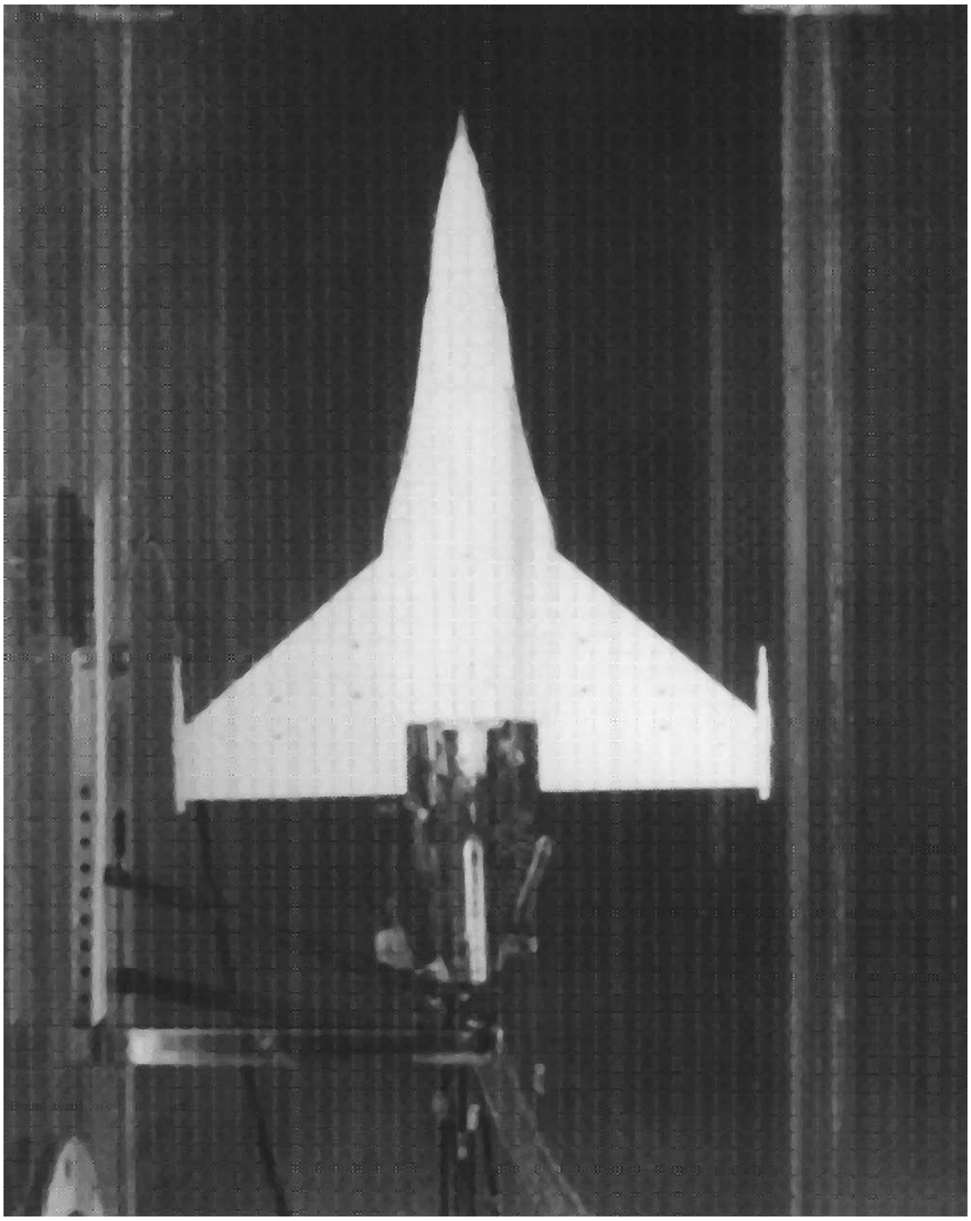

EC9442399-7

(b) View from the yaw axis.

Figure 13. Concluded.

pitched to the model support system limits with no tunnel wall contact.

The second example consists of an 1 ⁄ 32 scale F-16 model. This model is 18 in. long with an additional 0.25-in. sting support attached from the model rear. The wingspan is 11.75 in. The wingtips include missile launcher rails. This model could be pitched fully to 90°, but the yaw angle is limited to approximately 12° because the wingtip launcher rails come in contact with the walls of the tunnel.

Blowing and Suction

Certain tests require the ability to suck and blow water through openings on model aircraft. These openings simulate operational inlets and nozzles.[26] The FVF permits the user to control blowing and suction for a variety of tasks. Calibrated flow meters are used to measure the blowing or suction rates. Figure 14 shows a Harrier model and depicts the flow ingested by the inlets and expelled from the nozzles.

Moving Ground Plane

Certain tests require the absence of a ground plane boundary layer to model the flow properly.[26] An example would be a vertical or short takeoff and landing (V/STOL) aircraft hovering in close proximity to the ground with jet plumes impinging on the ground. In such tests, a moving ground plane is used in the FVF (figs. 15(a) and 15(b)). The moving ground plane is essentially a conveyor belt mounted on one of the narrow (16 in.) sides of the vertical test section. Fairings installed upstream of the belt promote smooth flow. The boundary layer generated on the wall and fairing ahead of the belt is removed at the leading edge of the belt by means of suction. Regeneration of the boundary layer on the belt surface is eliminated by operating the belt at free-stream velocity.

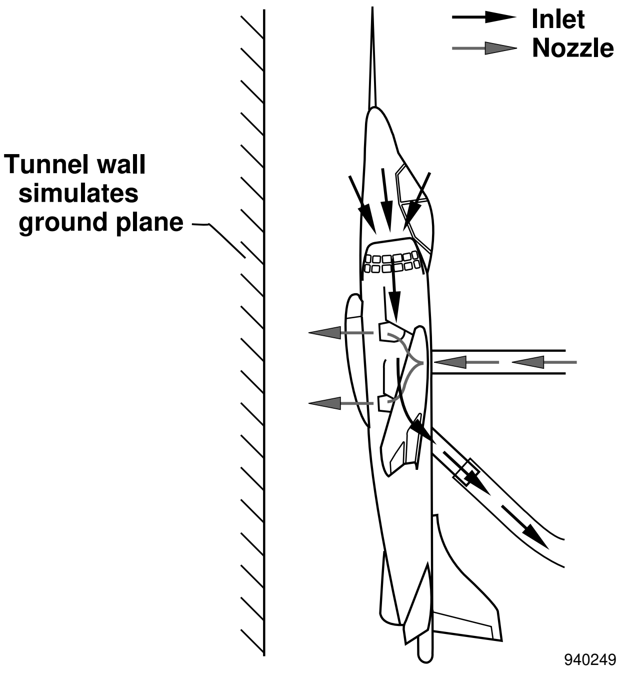
Inlet
Nozzle
Tunnel wall simulates ground plane
940249

Figure 14. Harrier model with blowing and suction capabilities.

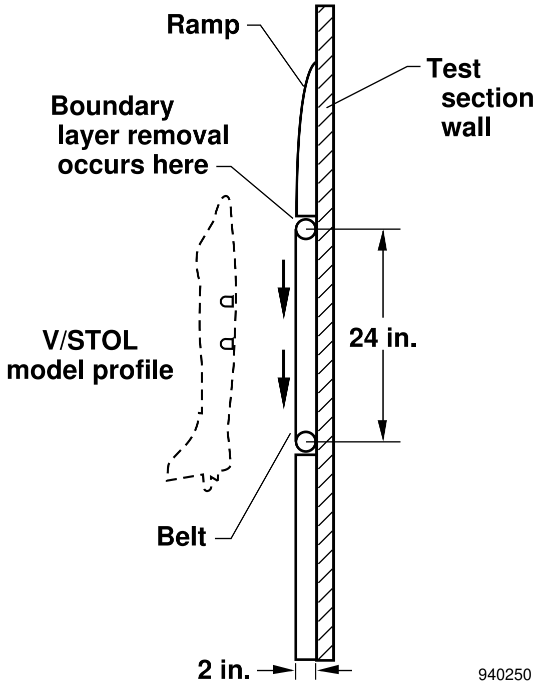
Ramp
Test section wall
Boundary layer removal occurs here
V/STOL model profile
24 in.
Belt
2 in.
940250

(a) Side view.

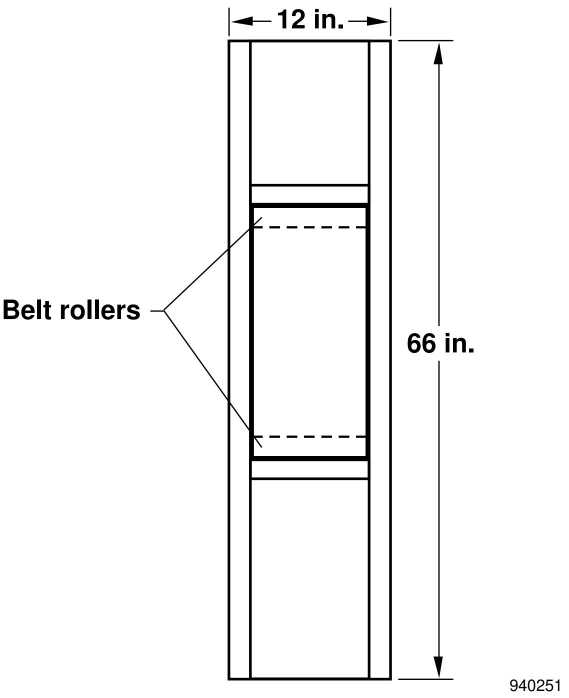
12 in.
Belt rollers
66 in.
940251

(b) Plan view.

Figure 15. Moving ground plane.

The transparent conveyor belt of the moving ground board assembly provides a view of the underside of model being tested and access for use of the laser light sheet. Dimensions of the area of the moving ground plane are 24 in. × 12 in. Other tests which require the absence of a boundary layer include ground vehicles, such as automobiles, trucks, and trains.

Cameras

Because the majority of the data generated in the FVF is visual, these data are usually recorded on video tape and as photographs. The video tape system consists of two video cameras, a video tape recorder, a unit which provides split-screen capability, and a video character generator. With this video system, one can simultaneously observe the top and side views of the model on the video monitor and insert test information onto the video signal being viewed and recorded. The test information created by the video character generator is typically used to identify the configuration, model position, date, and time. For photographic documentation, several 35mm and 120 film size cameras are available. A 16mm movie camera is also available.

MODELS

Loads imposed on models in the test section because of dynamic pressure are rather low. As a result, models need not be exceptionally strong. Many of the models built for use in the FVF start out as simple plastic hobby kits. Using commercially available kits increases the assortment of possible models which can be tested and helps keep the costs low. In-house model engineering and fabrication capabilities are available. Figures 16 through 18 show examples of models tested in the FVF.

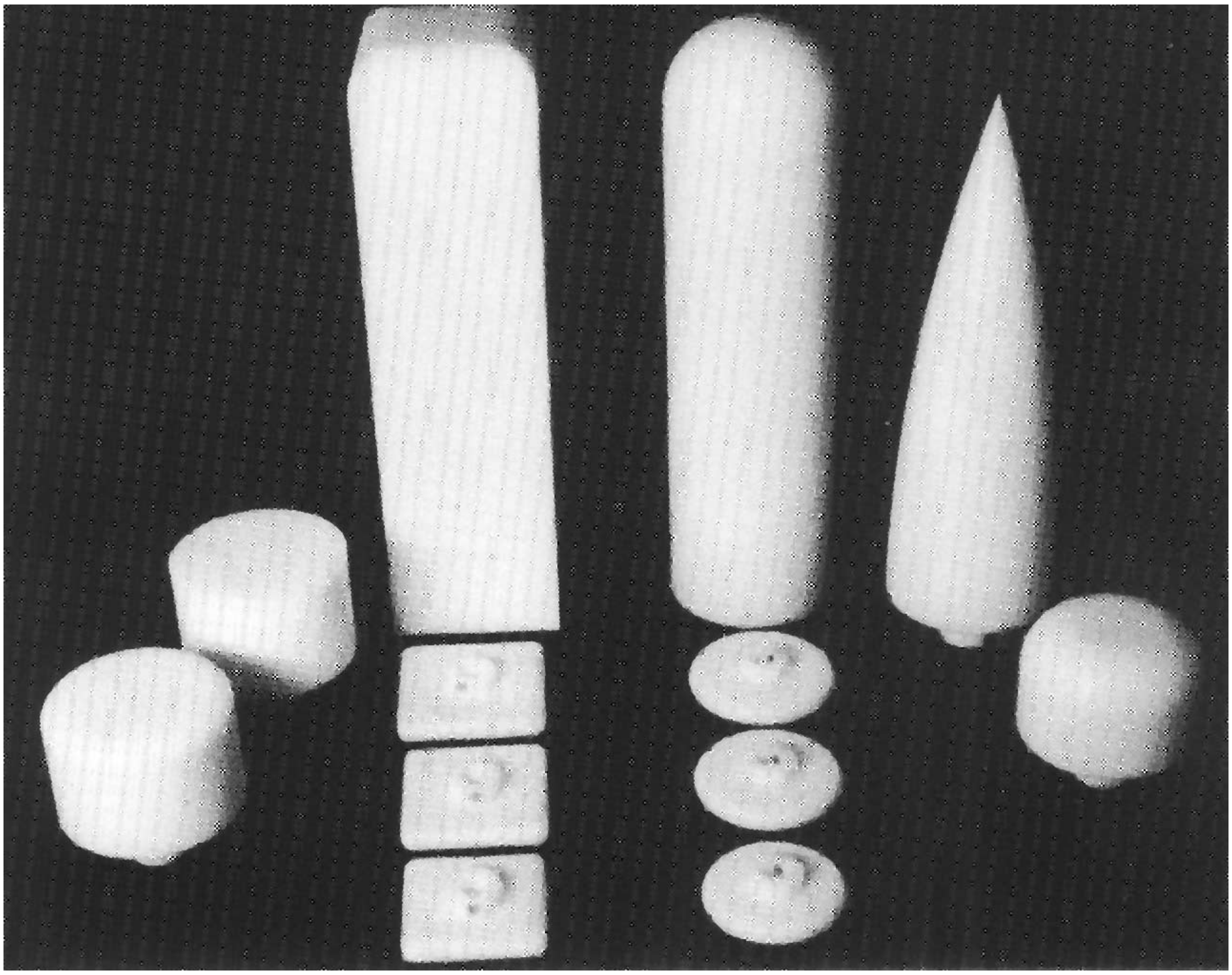

ECN32908

(a) Nose shapes, bodies, and disks used in the experiment.

Figure 16. Models used in a trailing disk experiment.

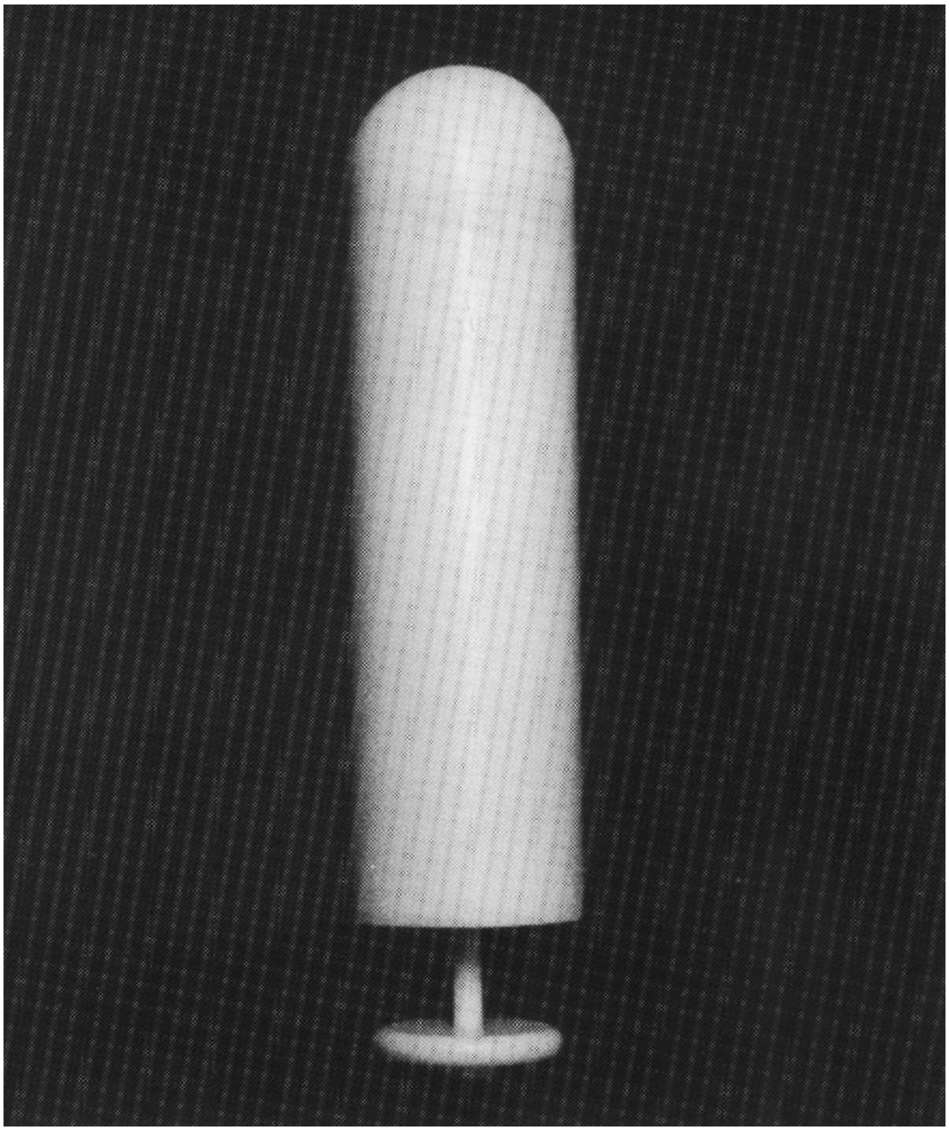

ECN32908

(b) Hemispherical nose with cylindrical body and disk.

Figure 16. Concluded.

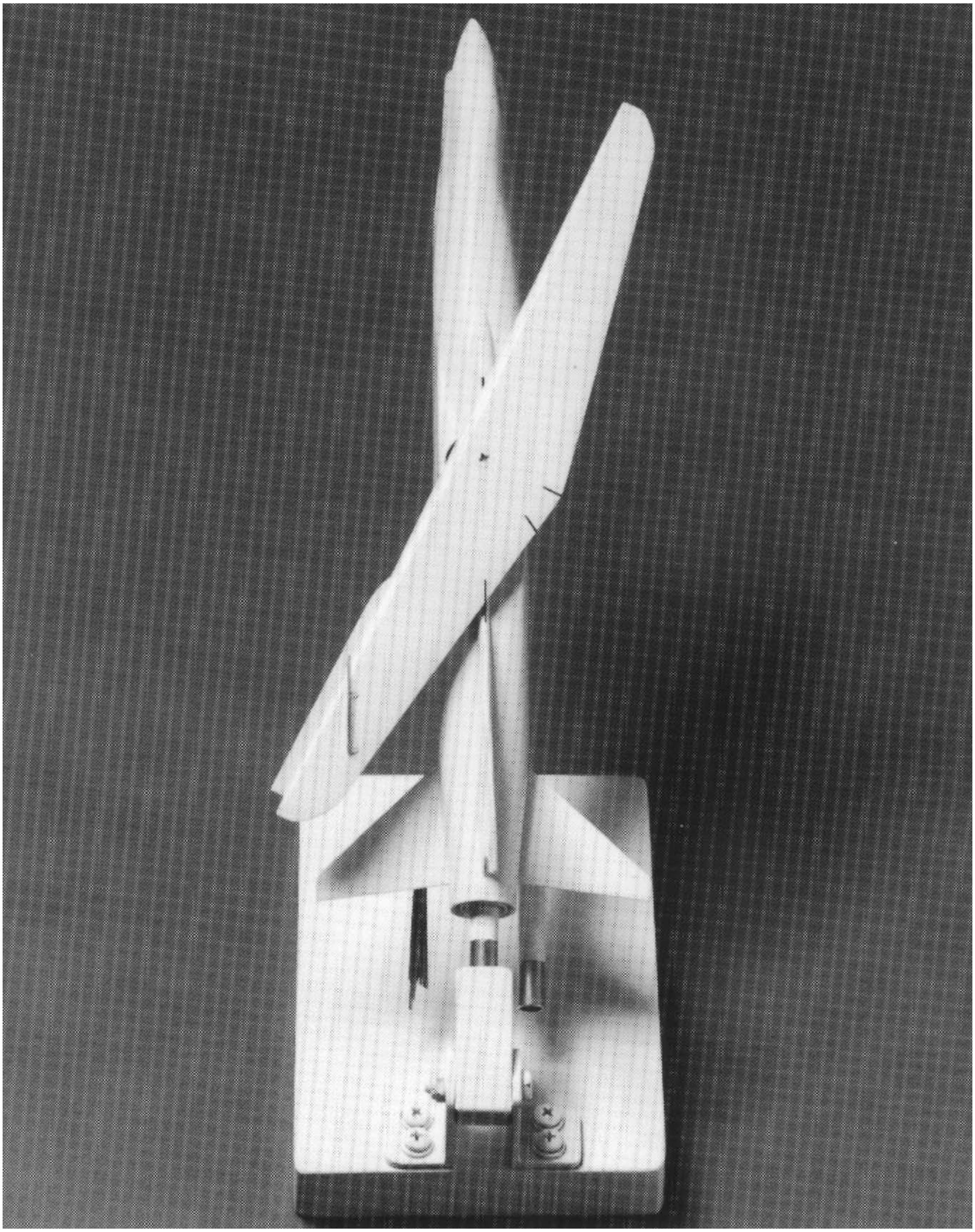

(a) Top view.

Figure 17. An F-8 oblique wind water tunnel model.

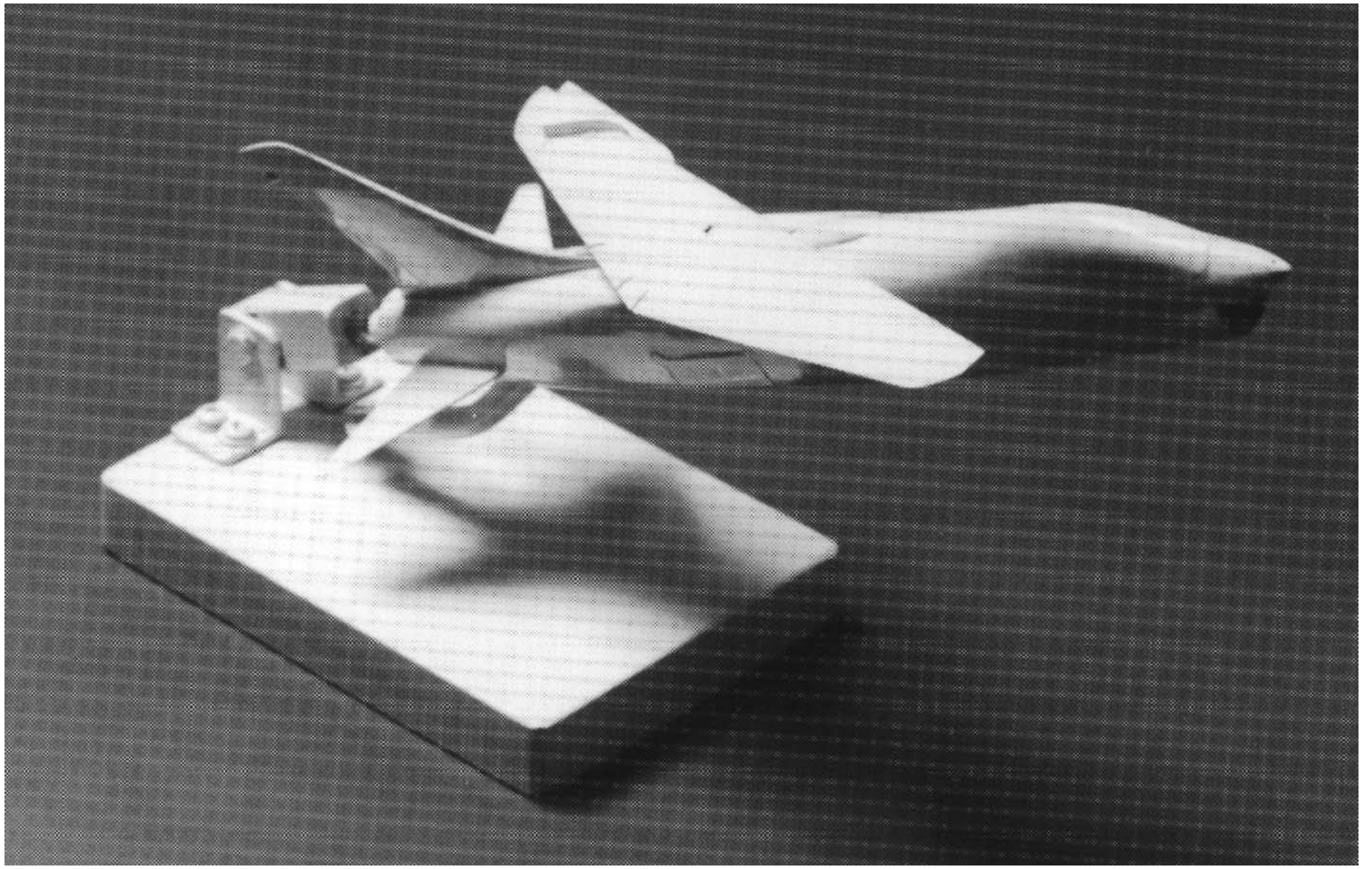

ECN31308

(b) Front quarter.

Figure 17. Concluded.

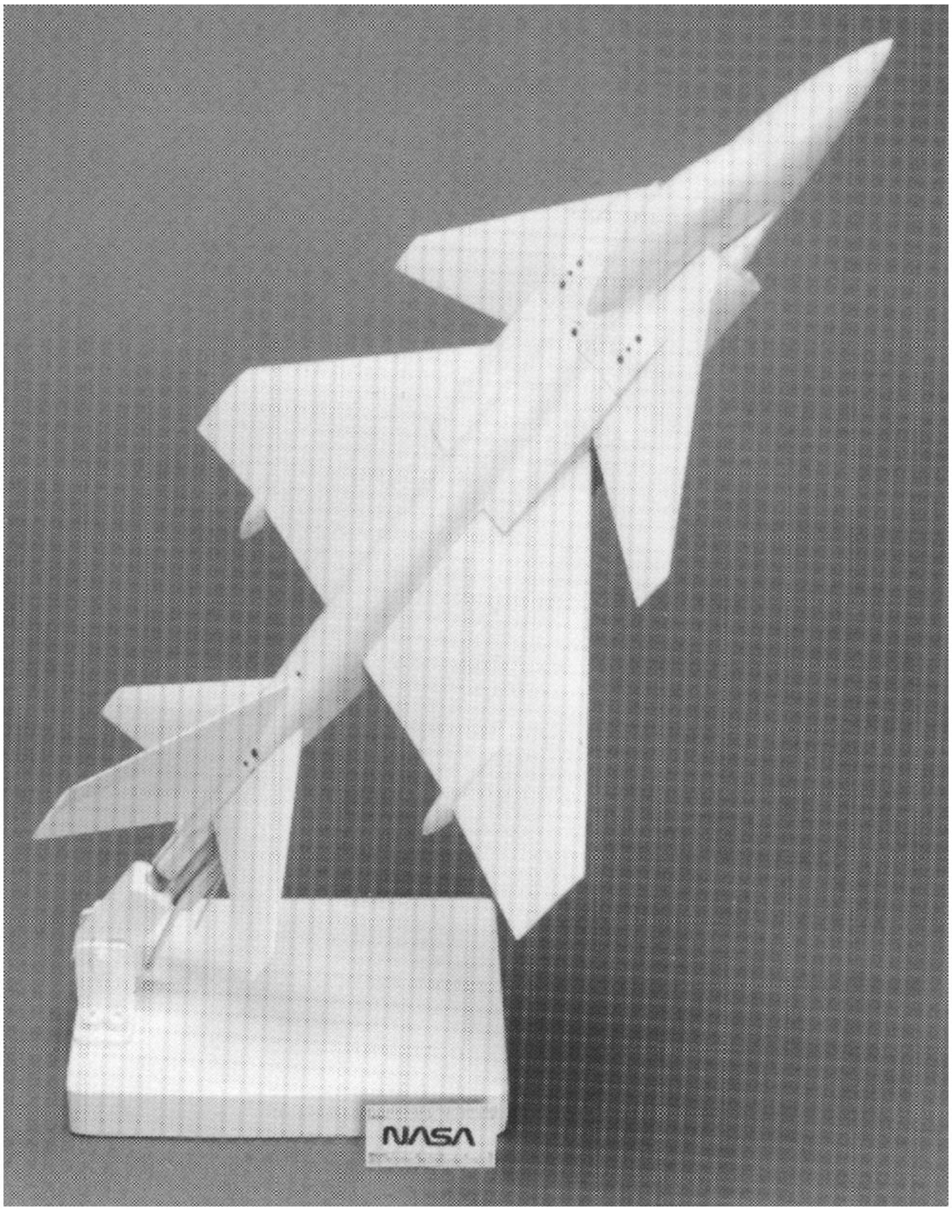

ECN33572-003

(a) Assembled.

Figure 18. MCAIR 279 water tunnel model.

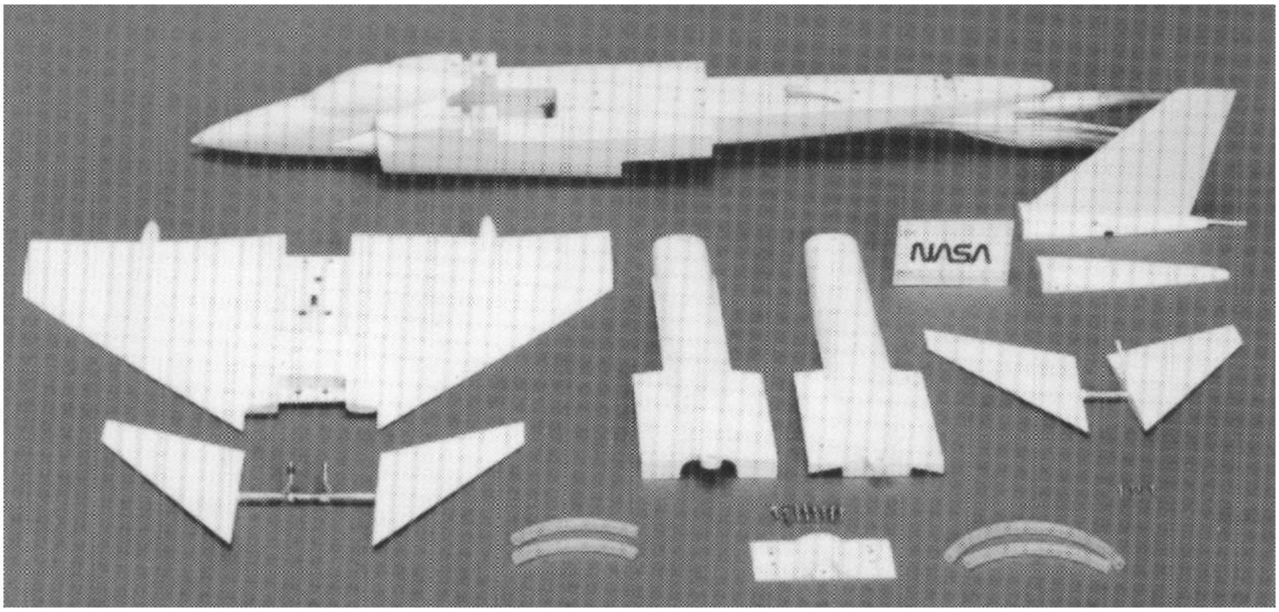

ECN33572-004

(b) Disassembled.

Figure 18. Concluded.

Models of 1 / 32 and 1 / 48 scale are typical for use with the standard model support system, but smaller models can also be used. Larger models are usually preferred because of ease of manufacture. Such models also provide increased fidelity, which yields more nearly accurate test results, and improved flow structure detail when compared to smaller ones.

FLOW VISUALIZATION FACILITY ENCLOSURE

The FVF resides in an enclosure designed specifically to house the facility. The enclosure provides restricted access necessary for testing classified models and using lasers. This enclosure consists of workshop, office, and storage areas as well as a high bay where the FVF stands.

FLOW VISUALIZATION FACILITY STAFF

The FVF is supported by experienced craftsmen and engineers. These personnel provide various levels of support which include designing, fabricating, instrumenting, installing, and testing models.

SUMMARY

Flow visualization of simple two-dimensional and complex three-dimensional vortical flows using water tunnels has proven its usefulness, in particular, as a flow diagnostic tool. Low-cost models and ease of operation allow researchers to study and evaluate many configurations quickly. The primary application of the facility is for flow simulations that are not highly Reynolds number sensitive, such as vortical flows from sharp edges.

The Dryden Flight Research Center Flow Visualization Facility, a closed-circuit water tunnel, can operate continuously. The vertical test section of the facility measures 16 × 24 × 72 in. Made of 2-in. thick clear acrylic plastic, this facility provides good visual access. This access is of paramount importance because the facility is used almost exclusively for flow visualization. Flow rates can be varied from 2 to 10 in/sec; however, a flow rate of 3 in/sec usually provides best results.

Colored dyes, emitted from the models or from probes, are usually used as the flow tracer. Multiple colors can be used simultaneously for flow identification. Other flow tracers include aluminum powder and fluorescent dyes. These materials are used less frequently than colored dyes. A laser light sheet is available for examining the flow cross-section and structure.

Typical aircraft models can be oriented in pitch ±90° and in yaw ±13° with the existing model support system. Specialized video and photographic equipment is available to document the flow visualization results.

Three quantitative measurement techniques have been employed at the Flow Visualization Facility to determine velocities. These techniques include laser doppler velocimetry, laser transit anemometry, and hot film anemometry. Hot film anemometry has also been used to determine flow turbulence and frequency content.

Access to the Flow Visualization Facility can be restricted for testing classified models and using lasers. The Flow Visualization Facility is supported by experienced craftsmen and engineers. The staff can provide various levels of support which include design, fabrication, instrumentation, installation, and testing. Such support capabilities offer the user a very broad experiment range.

APPENDIX
VERTICAL TEST SECTION CALIBRATION SYSTEM

This appendix describes the system used to calibrate the vertical test section of the water tunnel and the steps in processing the data. The measurements discussed here were taken to measure the vertical velocity component of the flow in the test section. The complete system consists of a hot film, wedge-shaped anemometer, which is supported in the water flow; a hot film constant temperature anemometer (CTA) unit; and a personal computer with signal processing software. Figure A-1 shows a schematic of the system.

The hot film probe support is routed through the test section door and was designed to sweep the probe across the test section centerline (fig. A-2). The probe was positioned at 10 locations along the centerline (figs. 4(a) and 4(b)). The measurements occurred 27 in. above the backflow screen.

The probe is the fourth arm of a Wheatstone bridge. The CTA control unit varies the current so that the temperature at the probe tip remains constant. The output voltage level is a function of the flow velocity. Output voltage was input to a personal computer using a 16-bit analog-to-digital board. Data are recorded and processed by a personal computer using customized software developed with a software package called LabVIEW II (National Instruments, Austin, Texas).

A typical run consists of setting the pump revolutions per minute at a particular setting and allowing the flow to stabilize for approximately 5 min. Then, the flow velocity is determined by releasing small pulses of dye at the centerline upstream of the hot film probe and timing these pulses over a 24-in. stretch. Four readings are taken, and an average value of the dye pulse speed, Vel', is recorded for each pump revolutions per minute setting. Immediately following the timing of the dye pulses, a 10-sec average of the hot film probe output voltage level, Vo', from the CTA is recorded. The dye pulse speed and the output voltage would later become part of the overall calibration curve. Next, the probe is stationed at each of the 10 locations (figs. 4(a) and 4(b)). Then, 10 sec of data from the CTA are recorded at each location. The output voltage from the CTA is recorded at 500 samples/sec.

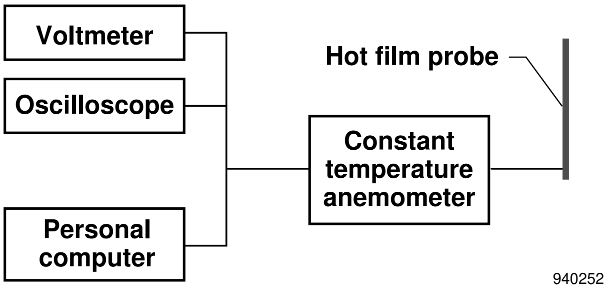

Figure A-1. Hot film constant temperature anemometer system assembled for use in the Flow Visualization Facility.

This procedure starts at the highest pump revolutions per minute setting of 550 and decreases sequentially through 500, 400, 300, 200 to 100 rpm. The complete range of pump settings is measured as quickly as possible because the hot film anemometer is sensitive to changes in water temperature. A temperature change causes a shift in the calibration curve. A complete calibration sweep through the test section takes approximately 50 min with runs at each speed setting taking approximately 8 min/run. The water temperature during measurements at any particular revolutions per minute setting changes less than 0.4 °F. This change in temperature causes a minor shift in the calibration curve. Such shifts could give a maximum error in the flow velocity of 0.4 in/sec at the steep end of the calibration curve.

The velocity, Vel', of the flow at the centerline determined by the dye pulses is plotted as a function of output voltage of the probe at the centerline position for the whole operational range of the pump (100 to 550 rpm). This calibration curve is then used to determine the corresponding velocities for each of the 10 probe locations. The velocity, Vel_{avg}, at each probe position is calculated by taking the average of each 10-sec sample group.

Using the same data and calibration curve, the percent of turbulence is determined at each probe position for all of the speed settings. The routine used by the signal processing software to determine percent of turbulence is described next.

1. The output voltage level from the CTA at a particular location is averaged over 10 sec and called Vo_{avg}.

2. The Vo_{avg} is subtracted from the output voltage which yielded the unsteady component of the raw voltage signal, $Vo_{unsteady}$.

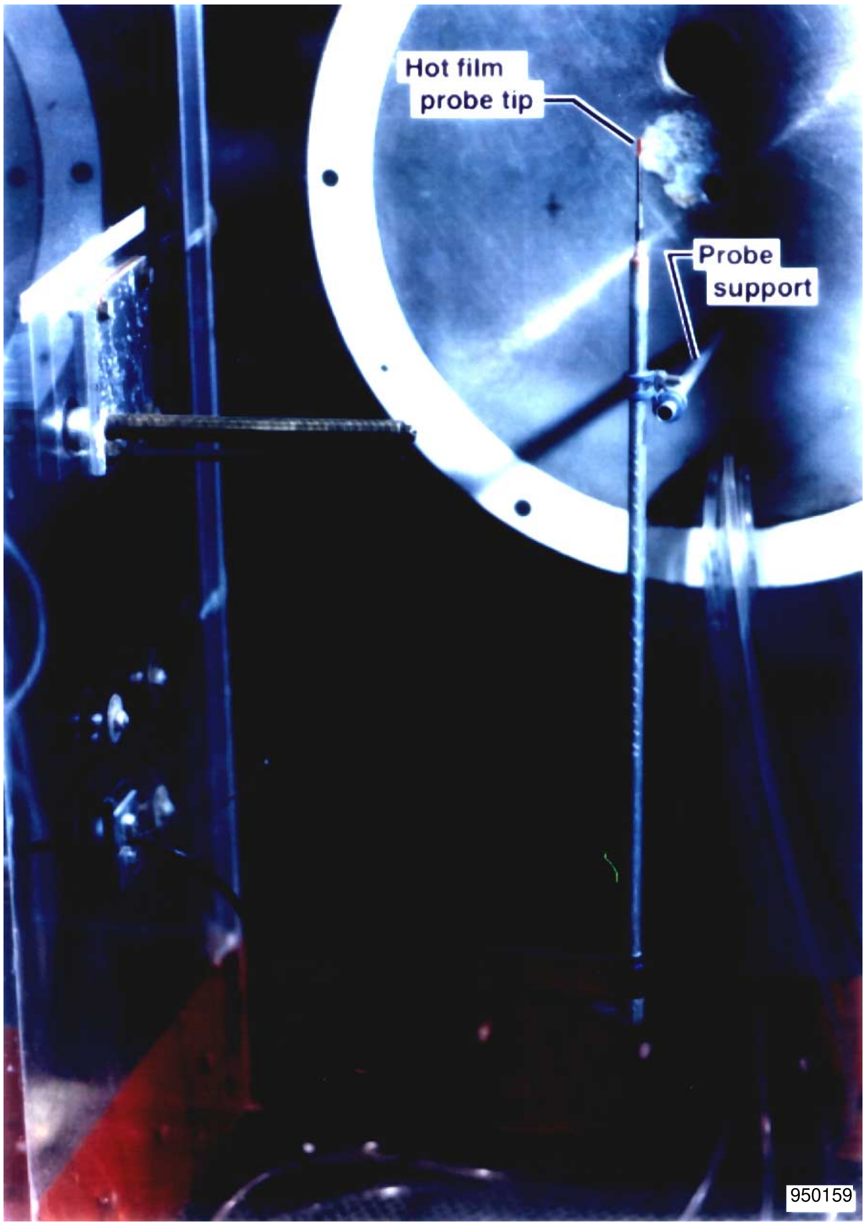

Figure A-2. Hot film probe installed in the vertical test section.

3. The slope of the calibration curve at Vel_{avg} is used to find the unsteady velocity, $Vel_{unsteady}$, component as shown in the following equation:

$$(Vo_{unsteady})\,(\mathrm{d}Vel'/\mathrm{d}Vo'\ (@\ Vel_{avg})) = Vel_{unsteady}$$

4. The turbulence intensity is determined by taking the root mean square of the $Vel_{unsteady}$ for each sample group (10 sec of data at 500 samples/sec yields 5000 samples in each sample group).

5. Percent of turbulence is determined by dividing the turbulence intensity by the Vel_{avg} and multiplying by 100 for each probe position.

REFERENCES

[1] Erickson, Gary E., "Vortex Flow Correlation," AFWAL TR-80-3143, Jan. 1981.

[2] Erickson, Gary E., David J. Peake, John Del Frate, Andrew M. Skow, and Gerald N. Malcolm, "Water Facilities in Retrospect and Prospect—An Illuminating Tool for Vehicle Design," AGARD CP-413, Oct. 1986. [Also available as NASA TM-89409, 1986.]

[3] Lorincz, Dale J., *A Water Tunnel Flow Visualization Study of the F-15*, NASA CR-144878, 1978.

[4] Lorincz, Dale J., *Space Shuttle Orbiter Flow Visualization Study*, NASA CR-163092, 1980.

[5] Lorincz, Dale J., *Flow Visualization Study of the HiMAT RPRV*, NASA CR-163094, 1980.

[6] Lorincz, Dale J., *Flow Visualization Study of the F-14 Fighter Aircraft Configuration*, NASA CR-163098, 1980.

[7] Del Frate, John H. and Fanny A. Zuniga, "In-Flight Flow Field Analysis on the NASA F-18 High Alpha Research Vehicle with Comparisons to Ground Facility Data," AIAA 90-0231, Jan. 1990.

[8] Holman, J.P., *Experimental Methods for Engineers*, 3rd ed., McGraw-Hill, New York, 1978, pp. 235–239.

[9] Werlé, H. and M. Gallon, "The New Hydrodynamic Visualization Laboratory of the Aerodynamics Division," *Rech. Aerosp*., no. 5, 1982, pp. 1–23.

[10] Werlé, H., "Liquids," and "Water Tunnel Testing," *Handbook of Flow Visualization*, edited by Wen-Jei Yang, Hemisphere Publishing Corporation, New York, 1989, pp. 41–44 and 409–413 (respectively).

[11] Merzkirch, Wolfgang, "Flow Visualization," 2nd ed., Academic Press, Orlando, 1987, pp. 17–24.

[12] Beckner, Christine and Robert E. Curry, *Water Tunnel Flow Visualization Using a Laser*, NASA TM-86743, 1985.

[13] Philbert, Michel, Jean Surget, and Claude Véret, "Light Sheet Technique," *Handbook of Flow Visualization*, edited by Wen-Jei Yang, Hemisphere Publishing Corporation, New York, 1989, pp. 211–217.

[14] Philbert, Michel, Jean Surget, and Claude Véret, "Shadowgraph and Schlieren," *Handbook of Flow Visualization*, edited by Wen-Jei Yang, Hemisphere Publishing Corporation, New York, 1989, pp. 189–201.

[15] Klein, Enrique J., "Interaction of a Shock Wave and a Wedge: An Application of the Hydraulic Analogy," *AIAA Journal*, vol. 3, no. 5, May 1965, pp. 801–808.

[16] Daily, James W. and Donald R.F., Harleman, *Fluid Dynamics*, Addison-Wesley, Reading, 1966, pp. 357–359.

[17] Orlin, W. James, Norman J. Lindner, and Jack G. Bitterly, *Application of the Analogy Between Water Flow with a Free Surface and Two-Dimensional Compressible Gas Flow*, NACA TN-1185, 1947.

[18] Ippen, A.T. and D.R.F. Harleman, "Studies on the Validity of the Hydraulic Analogy to Supersonic Flow—Part III," AF-TR-5985, Oct. 1950.

[19] Owen, F.K. and D.J. Peake, V*ortex Breakdown and Control Experiments in the Ames-Dryden Water Tunnel*, NASA TM-89410, 1986.

[20] Owen, F. Kevin, "A Laser Fluorescence Anemometer for Water Tunnel Flow Field Studies," *13th International Congress on Instrumentation in Aerospace Simulation Facilities*, Goettingen, Germany, Sept. 1989, pp. 298–309.

[21] Adrian, Ronald J., "Laser Velocimetry," *Fluid Mechanics Measurements*, edited by Richard J. Goldstein, Hemisphere Publishing Corporation, Washington, 1983, pp. 155–244.

[22] Trolinger, James D., "Laser Instrumentation in Aerodynamics," *SPIE's Technical Symposium Southeast on Optics, Electro-Optics, and Sensors*, Society of Photo-Optical Instrumentation Engineers, Washington, May 1987.

[23] Wentz, William H., Jr., "Vortex-Fin Interaction on a Fighter Aircraft," AIAA 87-2474-CP, Aug. 1987.

[24] Cunningham, A.M. and Todd Bushlow, "Steady and Unsteady Force Testing of Fighter Aircraft Models in a Water Tunnel," AIAA 90-2815, Aug. 1990.

[25] Suárez, Carlos J., Bert F. Ayers, and Gerald N. Malcolm, "Force and Moment Measurements in a Flow Visualization Water Tunnel," AIAA 94-0673, Jan. 1994.

[26] Kuhn, Richard E., John H. Del Frate, and James E. Eshleman, "Ground Vortex Flow Field Investigation," *1987 Ground Vortex Workshop*, NASA CP-1008, 1987.

REPORT DOCUMENTATION PAGE	Form Approved OMB No. 0704-0188

Public reporting burden for this collection of information is estimated to average 1 hour per response, including the time for reviewing instructions, searching existing data sources, gathering and maintaining the data needed, and completing and reviewing the collection of information. Send comments regarding this burden estimate or any other aspect of this collection of information, including suggestions for reducing this burden, to Washington Headquarters Services, Directorate for Information Operations and Reports, 1215 Jefferson Davis Highway, Suite 1204, Arlington, VA 22202-4302, and to the Office of Management and Budget, Paperwork Reduction Project (0704-0188), Washington, DC 20503.

1. AGENCY USE ONLY (Leave blank)	**2. REPORT DATE** May 1995	**3. REPORT TYPE AND DATES COVERED** Technical Memorandum

4. TITLE AND SUBTITLE NASA Dryden Flow Visualization Facility	**5. FUNDING NUMBERS** WU 505-59-53
6. AUTHOR(S) John H. Del Frate	
7. PERFORMING ORGANIZATION NAME(S) AND ADDRESS(ES) NASA Dryden Flight Research Center P.O. Box 273 Edwards, California 93523-0273	**8. PERFORMING ORGANIZATION REPORT NUMBER** H-1972
9. SPONSORING/MONITORING AGENCY NAME(S) AND ADDRESS(ES) National Aeronautics and Space Administration Washington, DC 20546-0001	**10. SPONSORING/MONITORING AGENCY REPORT NUMBER** NASA TM-4631

11. SUPPLEMENTARY NOTES

12a. DISTRIBUTION/AVAILABILITY STATEMENT Unclassified—Unlimited Subject Category 60	**12b. DISTRIBUTION CODE**

13. ABSTRACT (Maximum 200 words)

This report describes the Flow Visualization Facility at NASA Dryden Flight Research Center, Edwards, California. This water tunnel facility is used primarily for visualizing and analyzing vortical flows on aircraft models and other shapes at high-incidence angles. The tunnel is used extensively as a low-cost, diagnostic tool to help engineers understand complex flows over aircraft and other full-scale vehicles. The facility consists primarily of a closed-circuit water tunnel with a 16- × 24-in. vertical test section. Velocity of the flow through the test section can be varied from 0 to 10 in/sec; however, 3 in/sec provides optimum velocity for the majority of flow visualization applications. This velocity corresponds to a unit Reynolds number of 23,000/ft and a turbulence level over the majority of the test section below 0.5 percent. Flow visualization techniques described here include the dye tracer, laser light sheet, and shadowgraph. Limited correlation to full-scale flight data is shown.

14. SUBJECT TERMS Flow simulations; Flow visualization; Flow visualization instrumentation; High angle of attack; Vortex breakdown; Vortex flows; Water tunnel	**15. NUMBER OF PAGES** 30
	16. PRICE CODE AO3

17. SECURITY CLASSIFICATION OF REPORT Unclassified	**18. SECURITY CLASSIFICATION OF THIS PAGE** Unclassified	**19. SECURITY CLASSIFICATION OF ABSTRACT** Unclassified	**20. LIMITATION OF ABSTRACT** Unlimited

Available from the NASA Center for AeroSpace Information, 800 Elkridge Landing Road, Linthicum Heights, MD 21090; (301)621-0390